NANYANG
TECHNOLOGICAL
UNIVERSITY

Design of a Compact Wideband Antenna

Submitted by: S Sadiqa Mariam
Matriculation Number: U1522859F

Supervisor: Professor Shen Zhongxiang
Co-supervisor: Associate Professor Arokiaswami Alphones

School of Electrical & Electronic Engineering

2019

Table of Contents

Abstract

In the current technological climate, mobile devices have become an intrinsic part of how society functions. There is also an increasing trend and demand for these devices to be compact. As a result, there is a need for smaller electrical components that can fit seamlessly into these devices and antennas are an example of such components.

While small antenna design is imperative in the current industry, there is still much discourse about existing designs as performance degradations arise with the reduction in the size of the antenna.

This report will provide an insight on the designing of a compact wideband antenna. It will detail the design and simulation of a novel bowtie dipole antenna that operates within the Ultra-High frequency band. The antenna will be designed using a software known as High Frequency Structure Simulator (HFSS) and the results of the simulations will be presented and discussed in the following report.

Acknowledgements

I would like to take this opportunity to express my gratitude to those who have guided and supported me through the course of this project.

Firstly, I would like to thank my project supervisor, Professor Shen Zhongxiang, for giving me the opportunity to work on this final year project. I appreciate him taking time off his busy schedule to offer me the guidance and knowledge to help me along with the project.

Secondly, I would like to express my gratitude to my project examiner, Associate Professor Arokiaswami Alphones, for taking the time and effort to assess my performance on this project.

Thirdly, I would like to thank PhD candidate, Mr Huang Hao, for helping me with issues I faced with the software.

Last but not least, I am deeply grateful for the motivation and support extended to me by my family and friends throughout the course of this project.

S Sadiqa Mariam

November 2019

List of Figures

List of Tables

Chapter 1

Introduction

1.1 Background

In recent years, leaps in technological advancement have allowed the mobile devices industry to flourish and produce multiple new devices, for various purposes, at a rapid rate. There is currently an increasing demand for these devices as they greatly influence the way that present day society functions [1]. There is also a marked preference for such devices to be sleek and small-sized, so that users can hold, use and store the item with convenience. These devices, due to their diminished physical sizes, require electrical components that are reduced in size as well. An antenna is an example of an electrical component that performs a crucial function in most mobile devices.

Antennas are metallic structures that perform the function of transmitting and receiving waves of an electromagnetic nature [2]. In mobile devices, a receiving antenna acts as a transducer that picks up energy being directed to it and relays that signal to a radio chipset. This signal will then be converted from an analogue signal to a digital one. This signal will then be available for use by the main processor of the device [3]. A transmitting antenna will perform the reverse operation. A typical smart device in this day and age will usually contain multiple antennas. These antennas are necessary for Wi-Fi, Bluetooth and Global Positioning Systems (GPS).

1.2 Motivation

The main motivation behind carrying out this project is the relevance that the design of small antennas holds in the current technological climate. There is a mounting interest in the field of small antennas design due to the growing demand for smaller electrical components that can fit into compact mobile devices. Due to the large scale integration of electronic components, the antenna is often times isolated as the bulkiest and most obtrusive part of the equipment in most cases [4]. For instance, in modern wireless applications such as Radio Frequency Identification (RFID), the antenna is the biggest electrical component that is in use and as a result, it dictates the physical size of the particular device [5]. This shows the importance of reducing the size of the antenna used in such applications.

However, the designing of low-profile antennas remains an engineering challenge due to limitations that restrict the antenna from performing optimally following the reduction of physical size. These limitations will be examined further in Chapter 2 of this report. While small antennas are high in demand, there are multiple challenges that one has to overcome to achieve an optimally-functioning low-profile antenna [4], and this fact served as motivation for the undertaking of this project.

1.3 Objective and Scope

The objective of this project – the design of a compact wideband antenna – is to study a wideband antenna that is able to perform optimally whilst being small in physical size. The scope of this project comprises the study and design of a bowtie-shaped dipole antenna and the optimisation of its design to ensure that its performance meets the objective of this project. Simulations have been conducted using the software High Frequency Structure Simulator (HFSS), and this software will be further expounded in Chapter 3 of this report. The HFSS software is used to design a bowtie dipole antenna, after which alterations are made to the design to allow it to operate over the frequency range of 200 to 600 MHz. Following this, miniaturisation techniques are studied in order to reduce the size and profile of the proposed antenna.

1.4 Organisation of the Report

The following report comprises five chapters in total. Chapter one, in which the background, motivation, objective and scope of the project are discussed, serves as a precursor for the rest of the report.

Chapter two consists of a literature review of antenna basics. It will outline antenna parameters such as return loss, radiation patterns and gain and also include material about low-profile Ultra High-Frequency (UHF) antennas.

Chapter three introduces the HFSS software that has been extensively used in the course of this project. It will also present an examination of a bowtie dipole antenna design that has been formerly reported on.

Chapter four presents the design and simulation of the proposed antenna. It contains information about the structure of the antenna and the different results obtained after simulation.

Chapter five serves as the conclusion to the report. It summarises the work that has been conducted and holds recommendations for any avenues that can be explored in the future, with relation to this project.

Chapter 2

Literature Review

2.1 Antenna Basics

Antennas are passive devices that serve as a transition between guided electromagnetic waves in wires and electromagnetic waves radiating in free space [6]. They exist in the form of wires, rods or metal tubing.

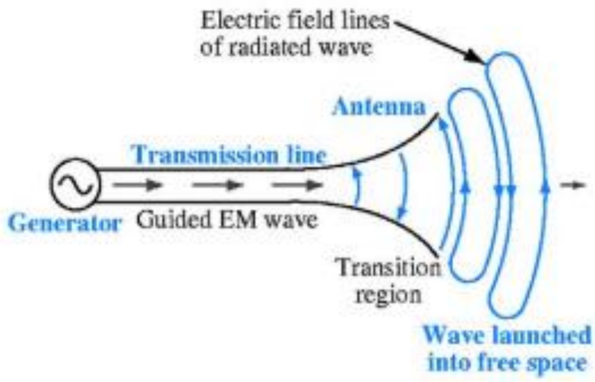

Figure 2.1: Radiating Antenna [7]

Since this transition is able to be done in either direction – transmission or reception – antennas are known to be reciprocal devices.

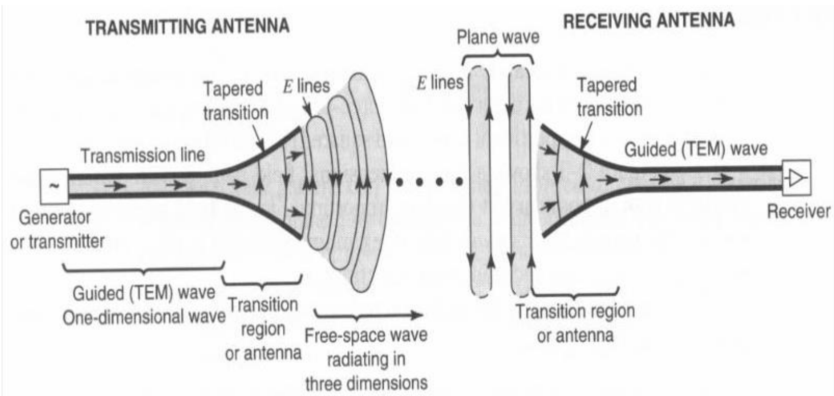

Figure 2.2: Reciprocal nature of an antenna [8]

Polarisation refers to the orientation of the electric field produced by an electromagnetic wave [9]. Polarisation can occur either linearly, circularly and the initial polarisation of a radio wave is decided by the antenna.

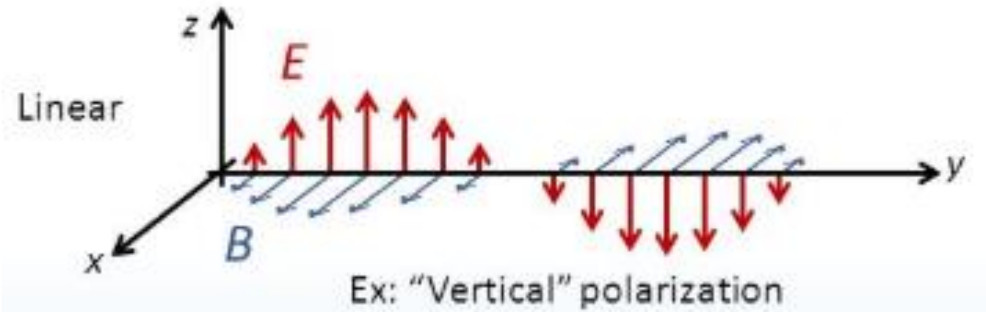

Figure 2.3: Linear Polarisation [8]

In the case of linear polarisation, the electric field vector exists in the same plane. Vertical polarisation, as shown in the above figure, is less influenced by reflections over the transmission line while for horizontal polarisation, these reflections can cause a discrepancy in strength of any received signals. Vertical antennas often-times pick up man-made interference as those are vertically polarised.

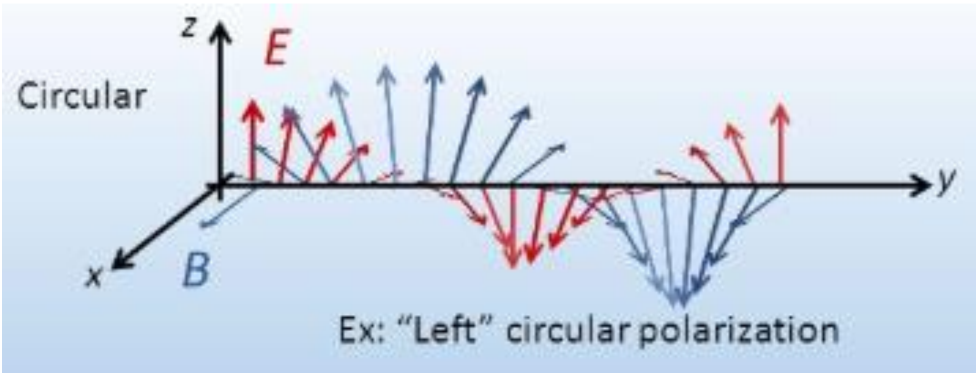

Figure 2.4: Circular Polarisation [8]

In the case of circular polarisation, the electric field vector rotates in a circular manner in around the propagation direction. Rotation can occur in a right or left manner and the latter is depicted in the figure above. Determining the polarisation of antennas is vital because if a transmitting and a receiving antenna do not have the same spatial orientation, same axial ratio and the same polarisation type, maximum power transfer would not be achievable [6].

When a polarisation mismatch exists between transmitting and receiving antennas, there is a loss in the power transfer between the antennas. This results in an overall degradation to the antenna system's efficiency and performance abilities.

Even if the antennas are of the same polarisation, a misalignment in how the antennas are mounted can also result in polarisation mismatch and the loss that arises due to this mismatch can be quantified using equation (1).

$$Polarisation\ Mismatch\ Loss = 20\,log(cos\Theta) \tag{1}$$

θ = misalignment angle between the transmit and receive antennas

Antennas exist in various shapes and sizes and these physical dimensions heavily influence the frequency in which these antennas can operate within and how they radiate electromagnetic waves [6]. Common types of antennas include log-periodic antennas, wire antennas, travelling wave antennas and microwave antennas. The chart below shows how different antenna types can be classified under these headings.

Table 1 Classification of antennas of different physical configurations

Log Periodic Antennas	**Wire Antennas**
• Bowtie Antennas • Log-Periodic Dipole Array	• Short Dipole Antenna • Dipole Antenna • Monopole Antenna • Loop Antenna
Travelling Wave Antennas	**Microwave Antennas**
• Helical Antenna • Yagi-Uda Antenna	• Rectangular Microstrip Antenna • Planar Inverted F-Antenna

Log-periodic antennas are directional antennas that can operate along a wide range of frequencies. These antennas have multiple elements which are dipoles placed along the axis of the antenna. These dipoles are spaced out following a logarithmic function of frequency, hence the name of the antenna [10]. These antennas are used when different bandwidths are required for different antenna gain and directivity values.

Figure 2.5: Log-periodic antenna [11]

Wire antennas are the most common types of antennas used for many applications due to their simplicity and affordability. Dipole antennas are well-known for being non-complex wire antennas. These antennas are made up of two thin metal rods that have a voltage difference. In addition to serving functions on their own, they also serve as components in the design of other antennas due to the fact that they are simple in nature.

Figure 2.6: Dipole antenna [12]

Yagi-Uda antennas are a form of travelling wave antennas used in many modern day applications due to their affordability and efficiency. They comprise of one or multiple reflector elements, a folded-dipole element and director elements. These are mounted such that there is horizontal polarisation.

Figure 2.7: Yagi-Uda antenna [13]

Microwave antennas refer to ones that operate at microwave frequencies. A rectangular micro strip antenna for instance, are used on aircrafts due to their reduced size, cost and weight. Such antennas only need space to fit their feed line and these feed lines can be attached behind the ground plane [10].

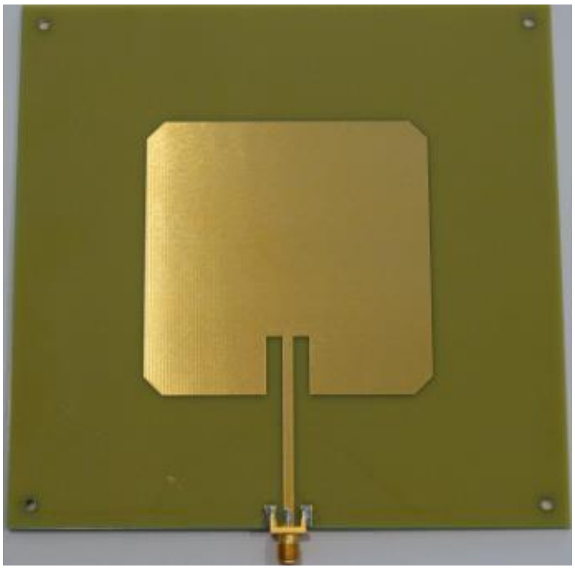

Figure 2.8: Microstrip Antenna

2.2 Antenna Parameters

Antenna parameters are essential for the study of the performance efficiency of antennas. The following are some parameters that are relevant to this project.

2.2.1 Reflection Coefficient

The Reflection Coefficient of an antenna (Γ) refers to the amount of power that is reflected from its load. It is also referred to as the S_{11} port parameter and is typically represented in dB. S_{11} quantifies the proportion of electromagnetic wave that is reflected by the impedance mismatch in the transmission medium [14]. There are multiple equations that can be used to calculate the reflection coefficient of an antenna and these are indicated below.

$$\Gamma = \frac{v_{ref}}{v_{fwd}} \tag{2}$$

V_{ref} = reflected voltage and V_{fwd} = forward voltage

$$\Gamma = \left| \frac{z - z_0}{z + z_0} \right| \tag{3}$$

Z_L = input impedance and Z_0 = characteristic impedance

$$\Gamma = \sqrt{\frac{P_{ref}}{P_{fwd}}} \tag{4}$$

P_{ref} = reflected power and P_{fwd} = forward power

Γ, in absolute value, will always lie between 0 and 1 as incident voltage is greater than reflected voltage in all cases due to the fact that there will at least be some amount of power transferred to the load antenna regardless of how poor the transmission line is matched [14].

2.2.2 Return Loss

Return Loss ($-S_{11}$) serves as a quantifier of how close the actual input or output impedance is to the nominal impedance value [14]. The equation to calculate Return Loss is as follows:

$$ReturnLoss = 10\,log_{10}\,\frac{P_i}{P_r} \tag{5}$$

P_i = Incident Power and P_r = Reflected Power

Inferring from the above equation, it can be seen that if all power is transferred to the load, the return loss would be infinite and if there is an open or short circuit scenario, all power is returned and hence, return loss would be 0 [14].

Since reflection coefficient is the ratio of the forward and reflected voltages, as depicted in aforementioned equation (2), and power is proportional to V^2, return loss and reflection coefficient are closely related:

$$ReturnLoss = 20\,log_{10}\,(\Gamma)) \tag{6}$$

Γ = Reflection Coefficient

Fig. 1 is a plot that shows the return loss (and by association, reflection coefficient) of a dipole antenna.

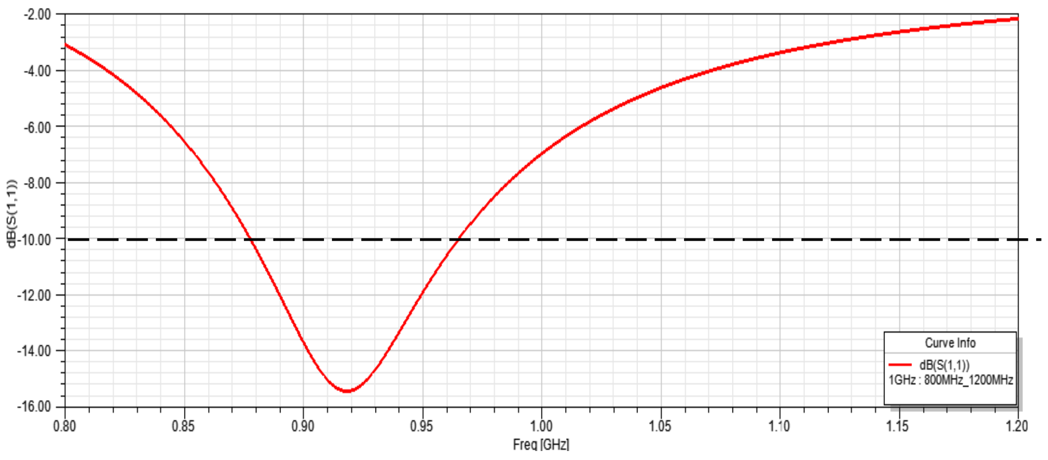

Figure 2.9: S-parameter plot of dipole antenna

Typically, -10 dB is set as the minimum threshold for S_{11} as it implies that only 10% of the incident power is reflected and that 90% of the power is transmitted into the antenna.

2.2.3 Voltage Standing Wave Ratio

The Voltage Standing Wave Ratio (VSWR) of an antenna measures the amount of power reflected from the antenna. As such, it is able to quantify the impedance match between the antenna and transmission line [15]. It can be calculated using the following equation:

$$VSWR = \frac{v_{max}}{v_{min}} = \frac{1+|\Gamma|}{1-|\Gamma|} \tag{7}$$

As can be seen from the above formula, VSWR is a function of the reflection coefficient and is the ratio between the maximum voltage and minimum voltage along the transmission line. VSWR can be of values that range from 1 to infinity. However, the lower the VSWR of an antenna, the lower the impedance mismatch between the antenna and transmission line.

The figure below shows an example of a VSWR plot.

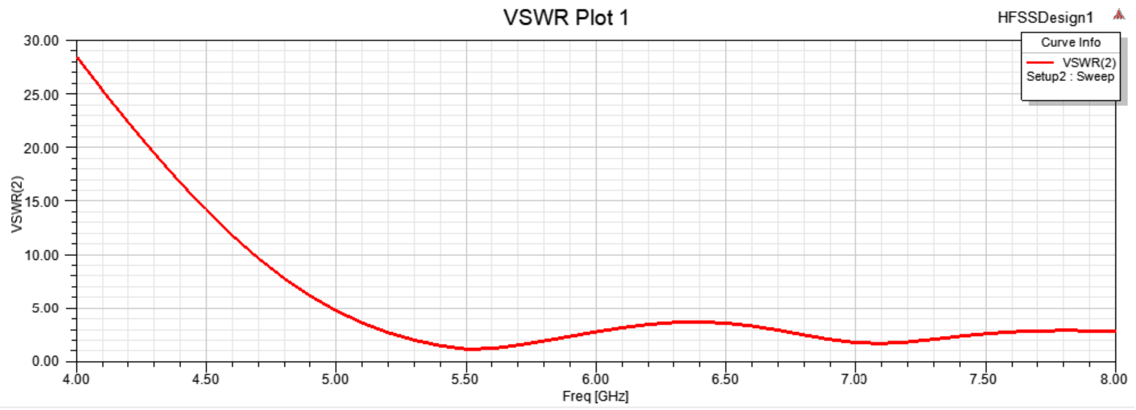

Figure 2.10: VSWR plot example

When the VSWR value is 1, there will be no power reflected and consequently, maximum power transfer is achieved. This would be the ideal case for any antenna, but a value under 2 is well-suited for most antenna applications [15].

2.2.4 Input Impedance

Antenna impedance, also known as radiation resistance, is the relation between voltage and current values at the input terminals of an antenna and it is a measure of the antenna's resistance to electrical signals [16]. The input impedance of an antenna fluctuates according to the frequency – be it low or high. The Z-parameter plot below depicts the input impedance of a dipole antenna plotted against frequency:

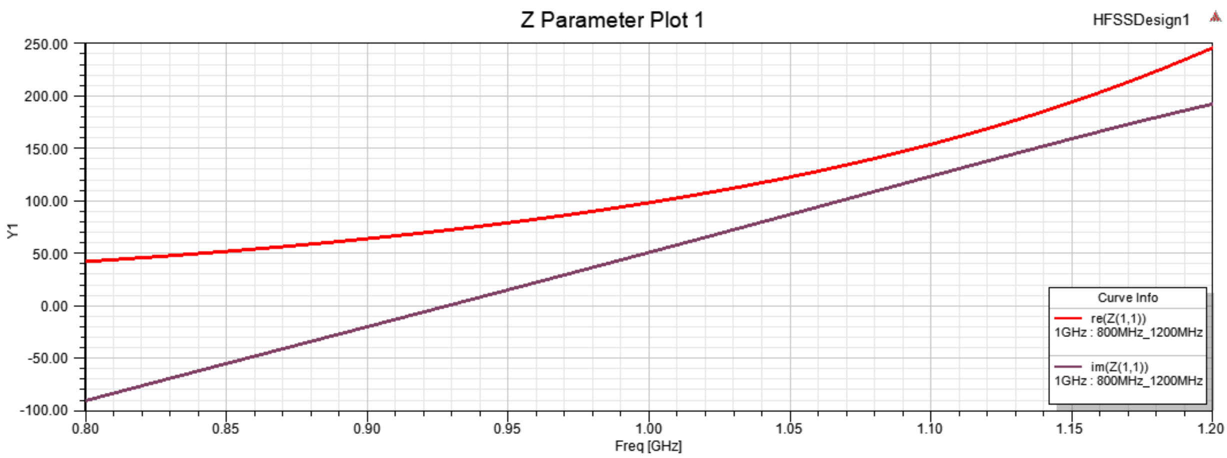

Figure 2.11: Z-parameter plot

As can be seen from Figure 3, input impedance has both real and imaginary values. The real part shows power that is radiated away from or absorbed into the antenna while the imaginary part shows power that is held in the antenna's near field (non-radiated power) [16]. When there is no imaginary part in an antenna's input impedance, the antenna is said to have a real input impedance. In this case, the antenna is known as a resonant antenna.

2.2.5 Radiation Pattern

Radiation pattern (F(θ, φ)) is a plot that displays energy radiated by an antenna [9] and it assists in the study of antennas by allowing a visualisation of an antenna's radiated energy as a function of direction. There are 3 different types of radiation patterns: isotropic, omnidirectional and directional, examples of which are shown in the following figures in 2D.

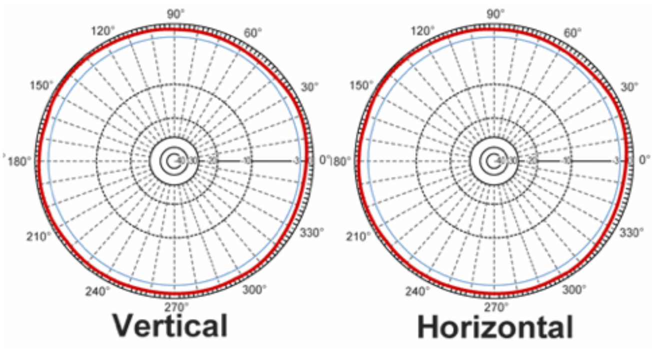

Figure 2.12: Isotropic radiation pattern [17]

Isotropic antennas radiate uniformly in all directions. It is impractical in real life and is only referred to as an ideal.

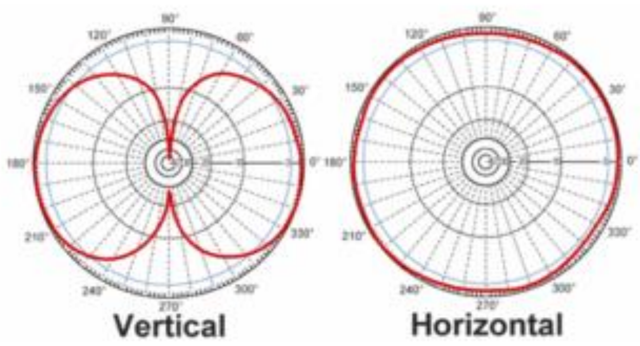

Figure 2.13: Omnidirectional radiation pattern [17]

Omnidirectional antennas form a figure-of-eight pattern in the vertical plane and radiate uniformly in the horizontal plane.

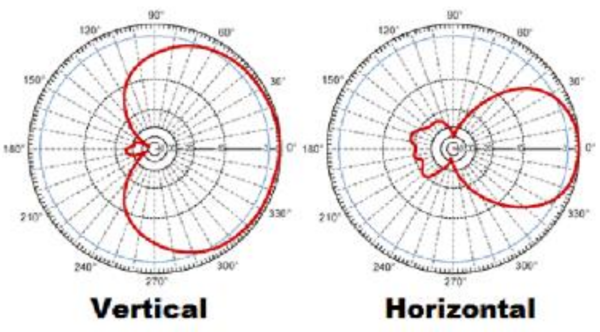

Figure 2.14: Directional radiation pattern [17]

Directional antennas radiate in a specific direction. This way, there is less interference from miscellaneous sources and performance is enhanced. As can be seen from figures 4 to 6, radiation patterns usually come in different shapes and the different protrusions are known as lobes. These lobes point out the major and minor radiation areas [9].

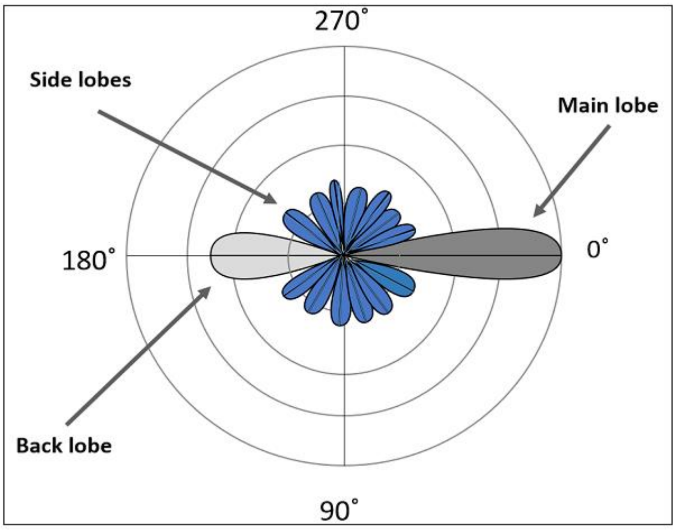

Figure 2.15: Lobe patterns

Figure 7 is the 2D radiation pattern for a dipole antenna. The main lobe shows the area in which there is maximum radiated energy. This is the lobe that one should look at when one wants to learn about the antenna’s directivity. The side lobes show the area in which energy is wasted. The minor lobe, which is located in a direction opposite to the main lobe, shows the area in which considerable amounts of energy is wasted [9].

Radiation patterns in 3D are oftentimes color coded to indicate different areas of intensity.

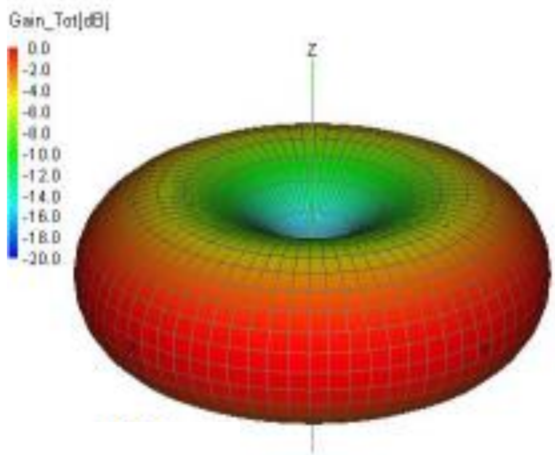

Figure 2.16: 3D radiation pattern plot

In the toroidal radiation pattern above, the red portions indicate that there is maximum radiation in the x-y plane and the green portion indicates that there is very little radiation along the z-axis.

2.2.6 Directivity, Gain and Antenna Efficiency

The directivity of an antenna measures the directionality of its radiation pattern [16]. Increased directivity denotes a more directional antenna. For instance, if an antenna's directivity is 1.2, the antenna receives 1.2 times more power in its peak direction, in relation to an isotropic antenna. Equation (8) can be used to calculate the directivity of an antenna.

$$D = \frac{1}{\frac{1}{4\pi}\int_{2\pi}^{0}\int_{\pi}^{0}|F(0,\Theta)|^2 \, sin\,\Theta \, d\Theta \, d\Phi} \tag{8}$$

The numerator would be the maximum value of F (radiation pattern) and the denominator would be the mean power radiated over all directions [16]. Cellular antennas are required to have low directivity as signals can arrive from any direction to the antenna.

$$\epsilon_R = \frac{P_{radiated}}{P_{in}} \tag{9}$$

An antenna's efficiency refers to the ratio between power being delivered to the antenna and the power being radiated from the antenna, as shown in the formula below [16]. A highly efficient antenna means that a high portion of power present at the antenna's input is radiated away.

Antenna efficiency losses can occur due to conduction losses, dielectric losses and impedance mismatch losses.

The gain of an antenna describes the amount of power that is transmitted in the direction of peak radiation, relative to an isotropic source [16]. For a receiving antenna with a gain of 6 dB in a specific direction, the antenna will receive 6 dB more power than an isotropic antenna that's lossless and the converse applies for a transmitting antenna. The formula to calculate gain requires the knowledge of the directivity and efficiency of the antenna in question.

$$G = \epsilon_R D \tag{10}$$

The gain of an antenna is desired to be low or high depending on how the antenna-mounted device will be used. If we have knowledge of where the desired signal will be coming from, a high gain would be desired and in the case that the signal will be arriving from various directions with relation to the antenna [16]. The latter applies for cellular antennas and GPS antennas as signals may be coming from various directions.

2.3 Frequency Spectrum

The frequency spectrum of an electrical signal refers to the distribution of the amplitudes and phases of each frequency component against frequency. Waveforms that contain information that needs to be sent is represented as the sum of a range of frequencies [16]. Modulation allows us to forward these waveforms to separate frequency bands. The set of all these frequencies is known as the frequency spectrum. The equation below, is a simple, yet often utilised one, which allows the determination of frequency.

$$f = \frac{c}{\lambda} \tag{11}$$

c = speed of light and λ = wavelength

The equation above will be used in a later part of the report to determine the width of an antenna element. In practise, the physical length of an antenna is referred to in relation to its wavelength and therefore, frequency is inversely related to the physical size of an antenna.

Table 2 below shows the different frequency bands together with their corresponding wavelengths and common applications.

Frequency Band Name	Frequency Range	Wavelength (Meters)	Application
Extremely Low Frequency (ELF)	3-30 Hz	10,000-100,000 km	Underwater Communication
Super Low Frequency (SLF)	30-300 Hz	1,000-10,000 km	AC Power (though not a transmitted wave)
Ultra Low Frequency (ULF)	300-3000 Hz	100-1,000 km	
Very Low Frequency (VLF)	3-30 kHz	10-100 km	Navigational Beacons
Low Frequency (LF)	30-300 kHz	1-10 km	AM Radio
Medium Frequency (MF)	300-3000 kHz	100-1,000 m	Aviation and AM Radio
High Frequency (HF)	3-30 MHz	10-100 m	Shortwave Radio
Very High Frequency (VHF)	30-300 MHz	1-10 m	FM Radio
Ultra High Frequency (UHF)	300-3000 MHz	10-100 cm	Television, Mobile Phones, GPS
Super High Frequency (SHF)	3-30 GHz	1-10 cm	Satellite Links, Wireless Communication
Extremely High Frequency (EHF)	30-300 GHz	1-10 mm	Astronomy, Remote Sensing
Visible Spectrum	400-790 THz (4*10^14-7.9*10^14)	380-750 nm (nanometers)	Human Eye

Table 2 Frequency bands and applications [16]

Antennas used in mobile systems operate within the frequencies of 300-3000 MHz and therefore, the scope of this project will focus on antennas in the Ultra High Frequency (UHF) band.

The bandwidth of an antenna is the range of frequencies over which the antenna can operate properly. An antenna's bandwidth is the number of Hz for which it will exhibit a Standing Wave Ratio (SWR) less than 2:1. The formula below describes how bandwidth and frequency are related:

$$BW = 100\,X\,\frac{F_H - F_L}{F_c} \tag{12}$$

F_H= highest frequency, F_L = lowest frequency, F_c = centre frequency

2.4 Ultra-High Frequency

Ultra-high frequency (**UHF**) refers to the label designated for radio frequencies (RFs) that range from 300 MHz to 3000 Mhz. UHF radio waves transmit largely by line of sight and ground reflection and there is very little reflection from the ionosphere. Their propagation is obstructed by hills and thus they are not able to travel beyond the horizon. However, such radio waves can go through foliage and buildings for the receiving of indoor signals. The illustration below depicts how UHF radio waves propagate:

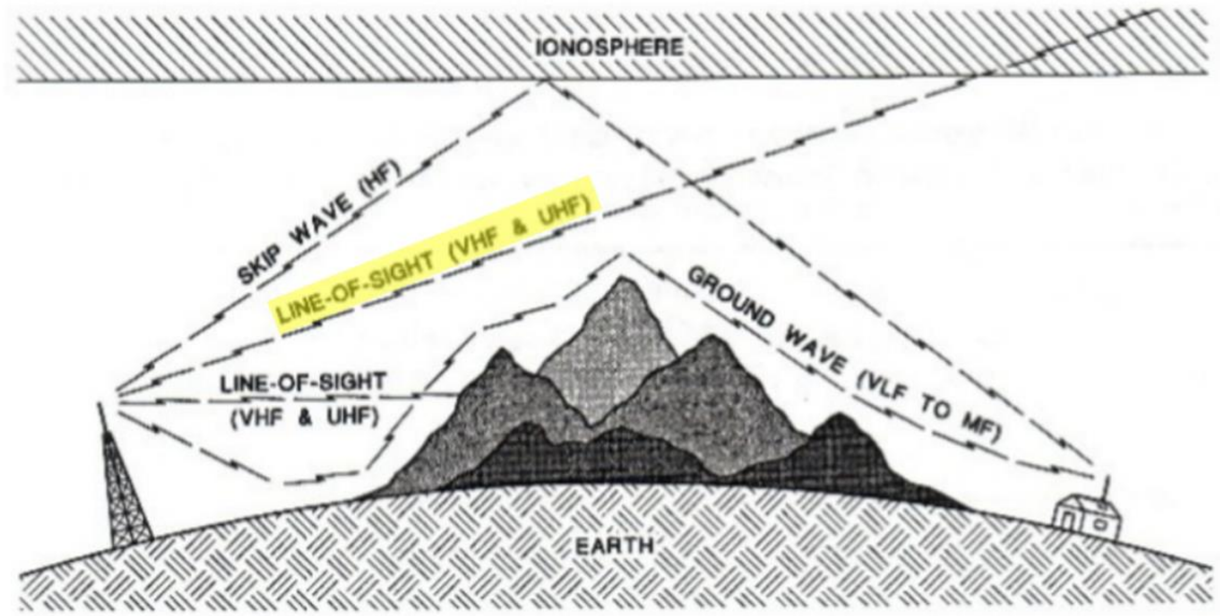

Figure 2.17: Propagation of UHF radio waves [18]

Since the length of an antenna is determined by the length of the radio waves, UHF antennas are stubby and short. This allows them to be mounted onto handheld and mobile devices. [19]

2.4.1 UHF low-profile antennas

UHF (ultra-high frequency) low-profile antennas are small antennas that operate in the 300-3000 MHz band of the frequency spectrum. The term “small” may hold different meanings with regard to antenna structures [4]:

1) **Electrically small antennas:** The largest dimension of the antenna less than $\lambda/10$, where λ refers to free-space wavelength. A short dipole antenna can be considered to be electrically small.
2) **Physically constrained antennas:** May or may not be electrically small. However, they are shaped in a manner that allows considerable size reduction to be attained in a single plane. Conformal antennas are examples of physically constrained antennas.

Figure 2.18: Conformal antenna

3) **Functionally small antennas:** May or may not be electrically small or physically constrained. An antenna is labelled functionally small if additional performance has been realised without an increase in the size of the antenna.
4) **Physically small antennas:** May or may not be a member of any of the aforementioned categories but are labelled as such if they are considered to be small in a relative sense. For example, a millimetre-wave horn antenna.

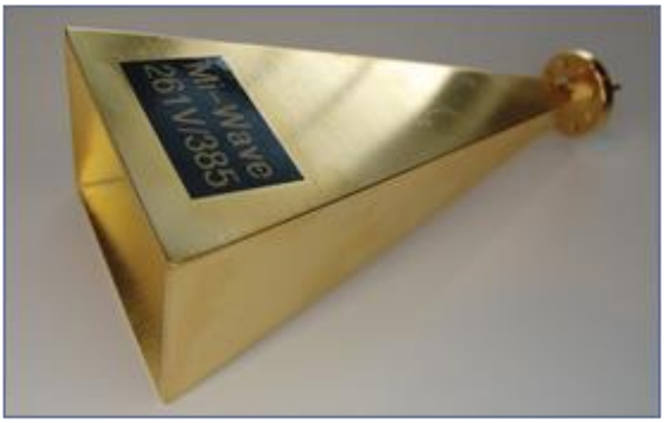

Figure 2.19: Millimeter-wave horn antenna

Low-profile antennas fall under the physically constrained antennas category [4]. As mentioned in chapter 1, there are several engineering challenges that one has to overcome in order to achieve an optimally-functioning UHF low-profile antenna.

2.4.2 Present Challenges

Antenna parameters are highly influenced by an antenna's physical size. The reduction in the physical size of an antenna causes a degradation in its performance. These performance penalties affect the bandwidth and efficiency of the antenna and as a result, impede the overall performance of the entire antenna system. There is thus a trade-off between antenna size, bandwidth and efficiency. This trade-off, however, is not straight-forwardly quantified. Small antennas can exist in several different types of shapes and sizes and have different system requirements. Therefore, the laws by which to predict the behaviour of these antennas, in general, are not simple and each antenna has to be examined individually according to its physical configuration and functional requirement. [4]

Fortunately, some trends in the trade-off between size and performance have been investigated and established. For one, it is recognised that smaller antennas have narrower bandwidths and poorer efficiencies compared to antennas that are bigger in size. [4]

2.4.3 Miniaturisation Techniques

The current proposed methods in order to overcome these existing challenges include using novel structures. This will involve designing an antenna structure that has an increased effective volume while the physical volume remains unchanged. This would lead to improved current distribution and a reduced near-field storage. Shown below is an example of a valentine antenna that has a novel physical configuration.

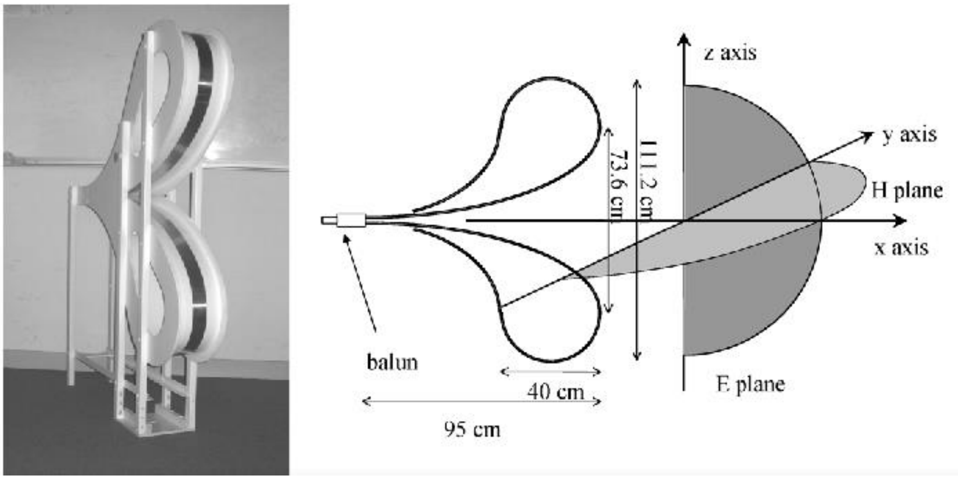

Figure 2.20: Valentine antenna [20]

Another method would be the loading of the antenna with materials. This will involve the loading of an antenna with dielectric materials in an effort to reduce its resonance frequencies. Loading materials such as magneto-dielectrics, meta-materials and anisotropic materials can be used to reduce an antenna’s resonance frequencies. This project will incorporate the study of both techniques to achieve a UHF low-profile antenna.

Chapter 3

HFSS Simulations

3.1 HFSS Software

During the course of this project, HFSS by ANSYS, was the main software used. It served as a useful tool for this project by providing a platform for the design of the antennas and allowing the simulation of the antennas to visualise its performance through plots and charts. This section will serve as an introduction to the functionalities of ANSYS HFSS. The following chart demonstrates the design checklist one needs to abide by when using HFSS to design and simulate an antenna.

Table 3 HFSS Design Checklist

Driven Solution	**Design**
Define the type of project ❑ Driven Modal ❑ Eigenmode	Construct the physical configuration of the antenna to be analysed.
Assign materials	**Assign Boundaries and excitations**
Assign materials to the physical components and assign substrate.	Assign radiation boundary and input a source of excitation for the model.
Assign solution set-up	**Analyse results**
Set up solution parameters, establish operating frequency and add a frequency sweep.	Solve the antenna and generate results of interest such as S-parameter and radiation pattern.

The general layout of the ANSYS HFSS window consists of a project manager, a message manager and a modeller window.

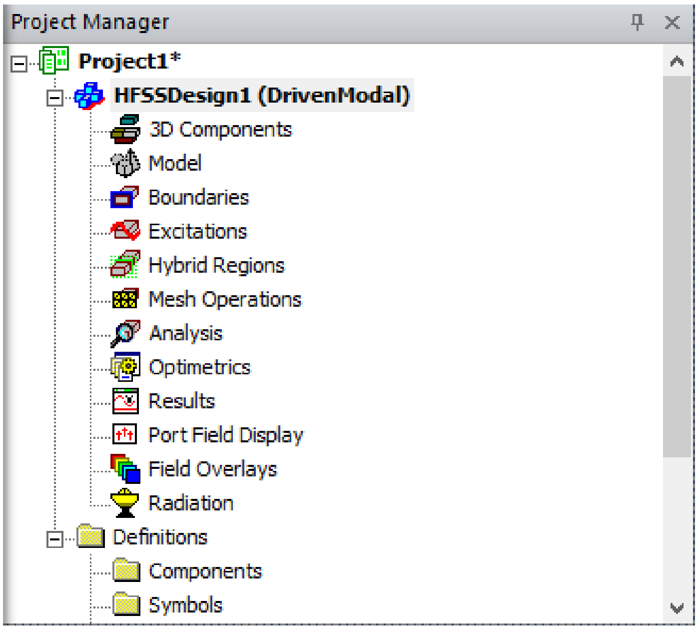

Figure 3.1: HFSS project manager

The project manager contains the project tree which shows all the components that contribute to the structure of the project.

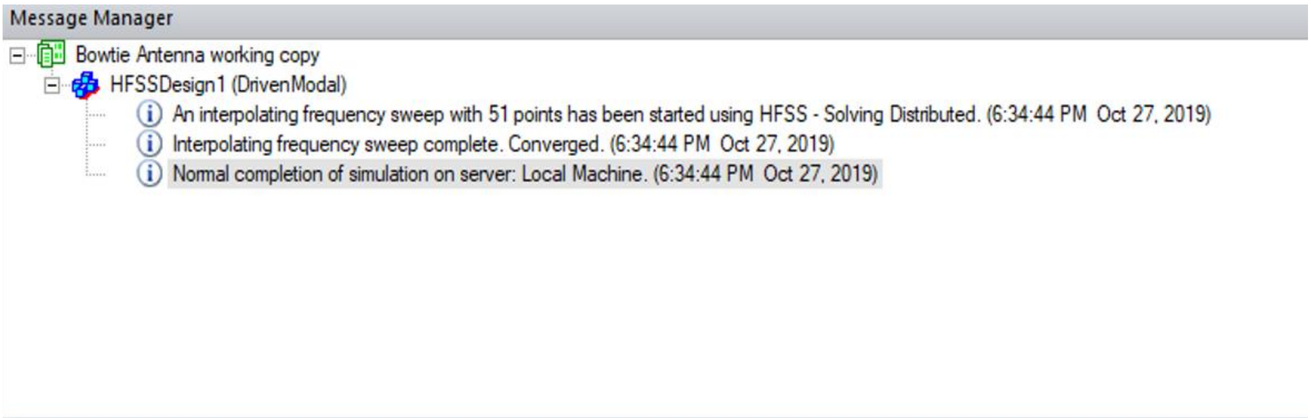

Figure 3.2: HFSS message manager

The message window notifies the user of any errors or warnings before or after simulation attempts.

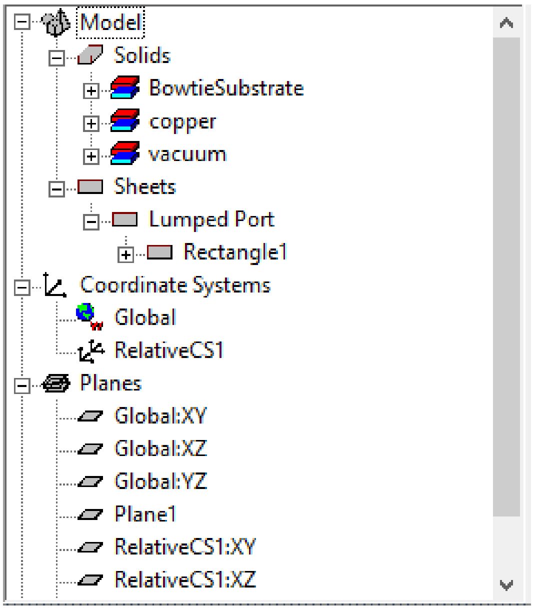

Figure 3.3: HFSS modeler window

The modeller window displays all the different components for the active design and any physical parameters can be changed using these tabs.

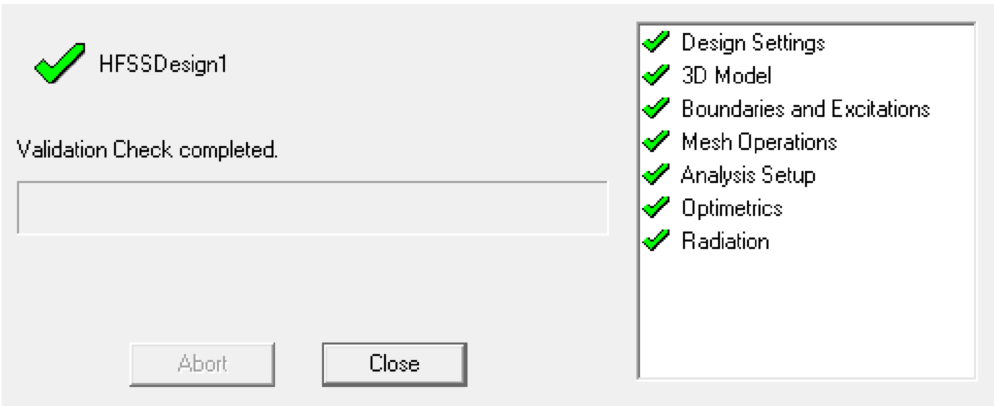

Figure 3.4: HFSS validation check

Once every design is completed and all materials and excitations have been assigned, one can check the validity of the design via conducting a validation check. Only after the checklist shown above has been completed can the antenna be solved to obtain results.

HFSS was extensively used to design and simulate the antennas for this project and the following chapters will detail that process and the results obtained.

3.2 Design Verification of Novel Bowtie Dipole Antenna

Bowtie antennas are subsets of biconical antennas [21]. Biconical antennas comprise of two close-to-conical conductive objects almost touching at the centre-point and Bowtie antennas are the two-dimensional version of that. The feed point for such antennas would be at the midpoint of the structure, where the two conductive objects almost touch.

Bowtie antennas are often used in UHF applications and have a wide bandwidth owing to its travelling wave structure. The figure below depicts how a Bowtie antenna typically looks like:

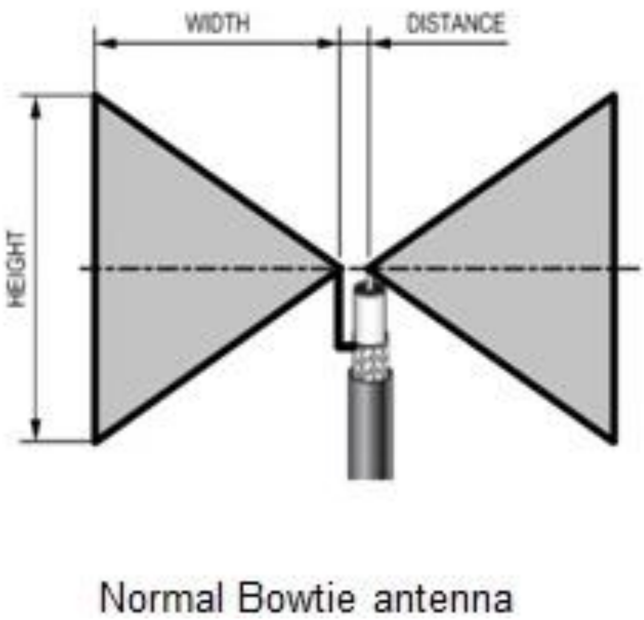

Figure 3.5: Bowtie antenna [27]

This section will detail the design process and simulation results of a novel bowtie dipole antenna. The results of this simulation will be compared with that of a parallel existing design that was designed for base station applications. The results of both the antenna designed for this project, and the reference antenna will be presented in the following section.

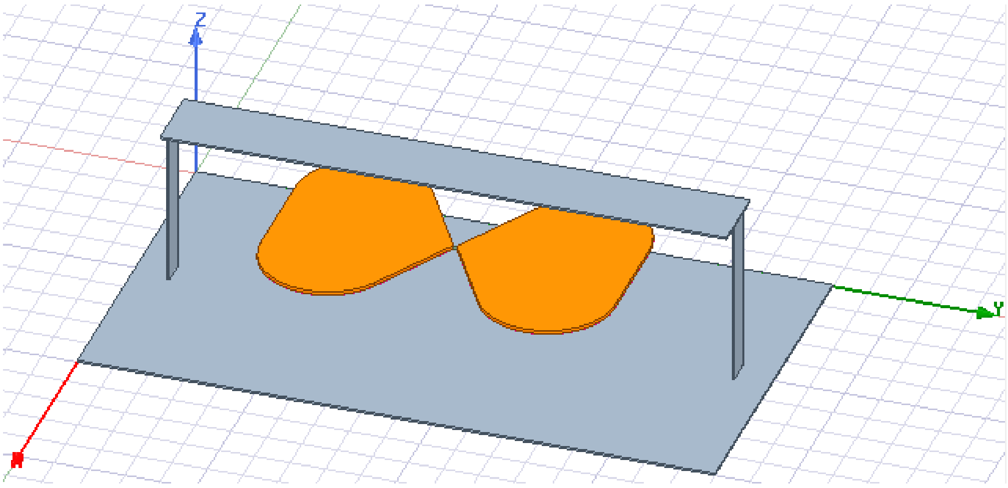

Figure 3.6: Novel bowtie dipole antenna design

The antenna set-up comprises of a bowtie dipole antenna with rounded corners, placed above a rectangular ground plane, with a metallic bridge set along the Y-axis. This design emulates one that has been formerly reported on. [22]

The geometry of the antenna designed above is as follows:

The rectangular ground plane is a 90 mm by 50 mm copper plate with a thickness of 0.3 mm. The metallic bridge is an 80 mm by 10 mm copper plate of thickness 0.3 mm. It is supported by 2 vertical supports of a lesser width than the bridge. These supports are 24.2 mm by 4 mm, of thickness 0.3 mm and have ends that are directly connected to the ground plane. Shown below is a clearer view of the ground plane and metallic bridge set-up, marked with their respective dimensions.

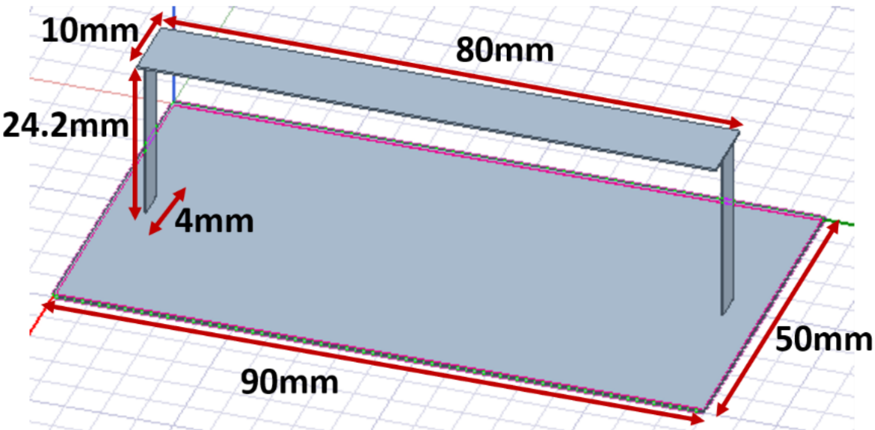

Figure 3.7: Dimensions of metallic bridge and ground plane

The bowtie element is made up of a regular triangular bowtie dipole with rounded corners. The element is fabricated on a substrate that has a thickness of 0.5 mm and a relative dielectric constant of 2.65. The height of the entire element is 27.45 mm, the flare angle is 120°, and the rounded corners are filleted with a radius of 9.5 mm. Studies show that these rounded corners not only lead to a reduction in antenna dimensions [22] but also contribute to improvements in the return loss and flatness of input impedance [23]. They also enhance the stability of radiation patterns [23]. Finally, the element is 12.5 mm above the ground plane.

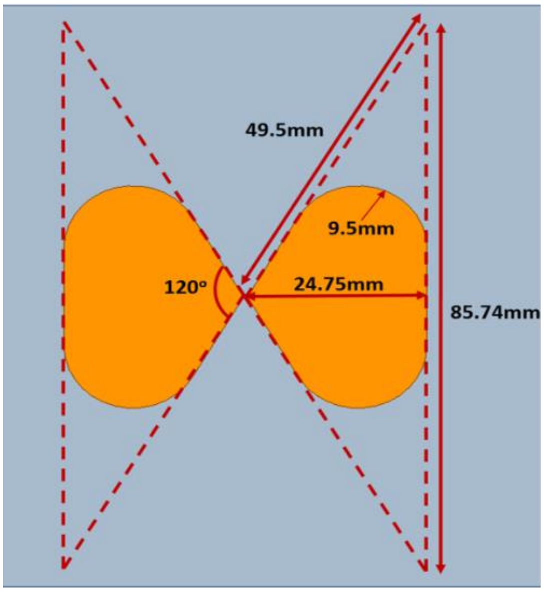

Figure 3.8: Dimensions of bowtie antenna

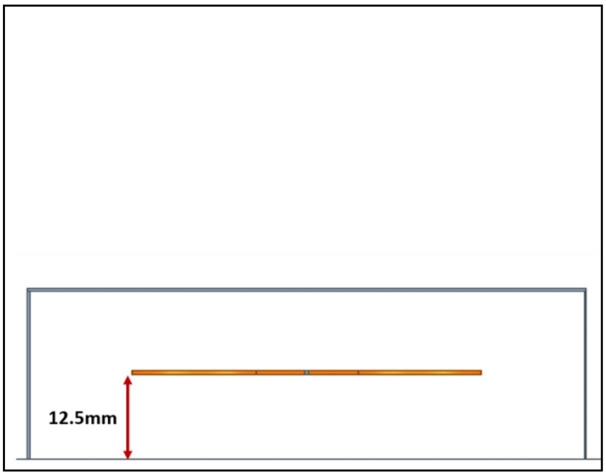

Figure 3.9: Height of bowtie relative to ground plane

The bowtie dipole antenna is assigned an excitation in the 0.5 mm gap between the right and left bowtie element. An ideal lumped port with characteristic impedance of 100 Ω is used. A lumped port can be used to excite an antenna and allow the computation of the frequency responses of the antenna [24].

To generate valid S-Parameters, a single excited lumped port is required. This type of port is typically applied on a tiny portion of the model and the port's boundary size should be small with respect to the operating frequency [24]. In this design, the port's dimensions are 0.5 mm by 0.5 mm. The port also has to be between two metallic conductors and be in contact with both these metallic surfaces in order to procure voltage.

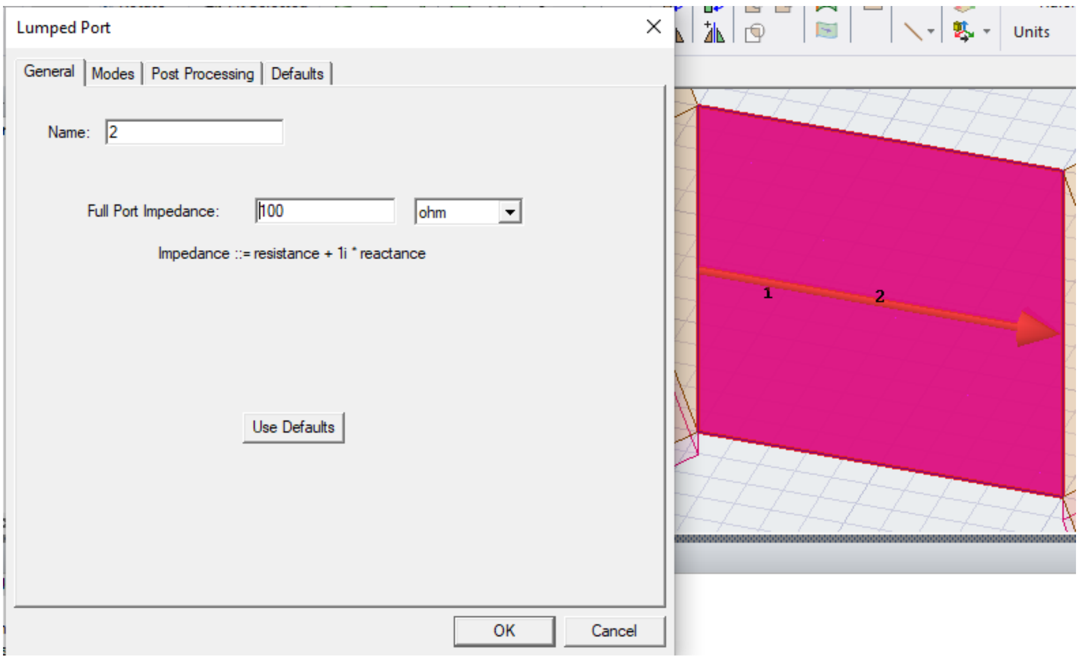

Figure 3.10: Lumped port excitation, integration line

Figure 3.10 shows the lumped port excitation in the gap of the bowtie elements. The line down the middle is the integration line defined. The integration line is the line were the E-field is integrated for procuring voltage. This line would be the deciding factor for the direction of the E-field.

The results of this antenna simulation yield the following results:

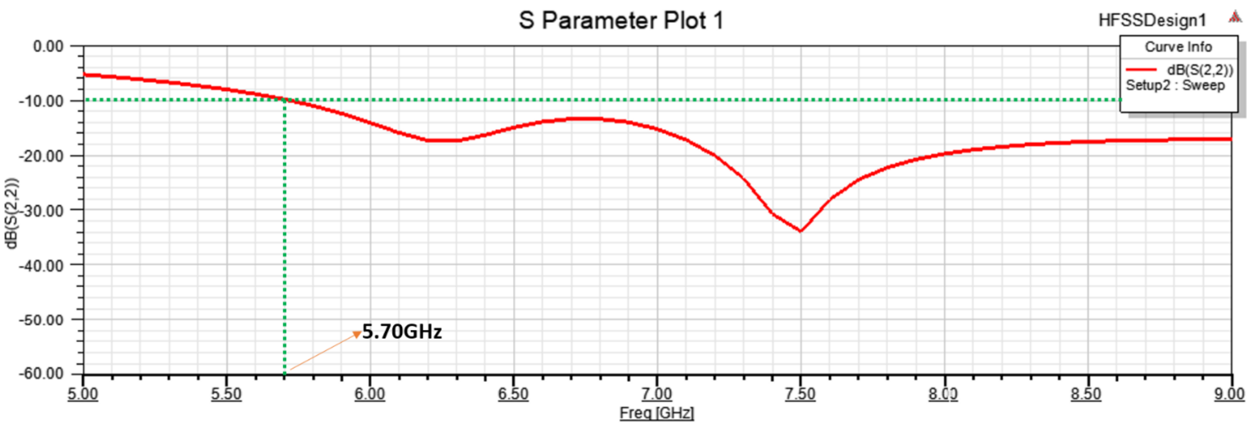

Figure 3.11: S-Parameter plot of bowtie dipole antenna

As can be seen from the above S-Parameter curve, the antenna has an acceptable return loss from 5.7 GHz.

This follows closely with the return loss results from the formerly reported on antenna that this design is based upon.

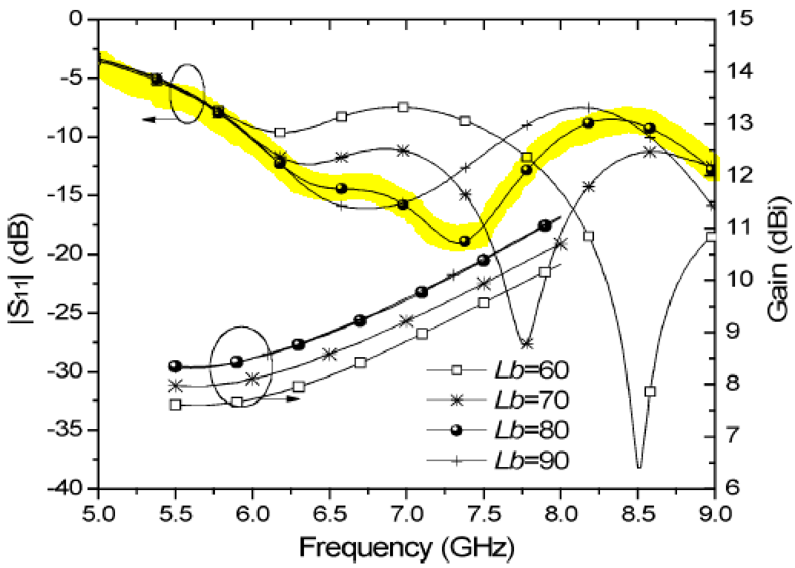

Figure 3.12: S-Parameter plot of reference bowtie dipole antenna

The highlighted curve would be the relevant one as that is the curve that corresponds to the length of the metallic bridge that has been used in the simulation for this project (L_b = 80 mm).

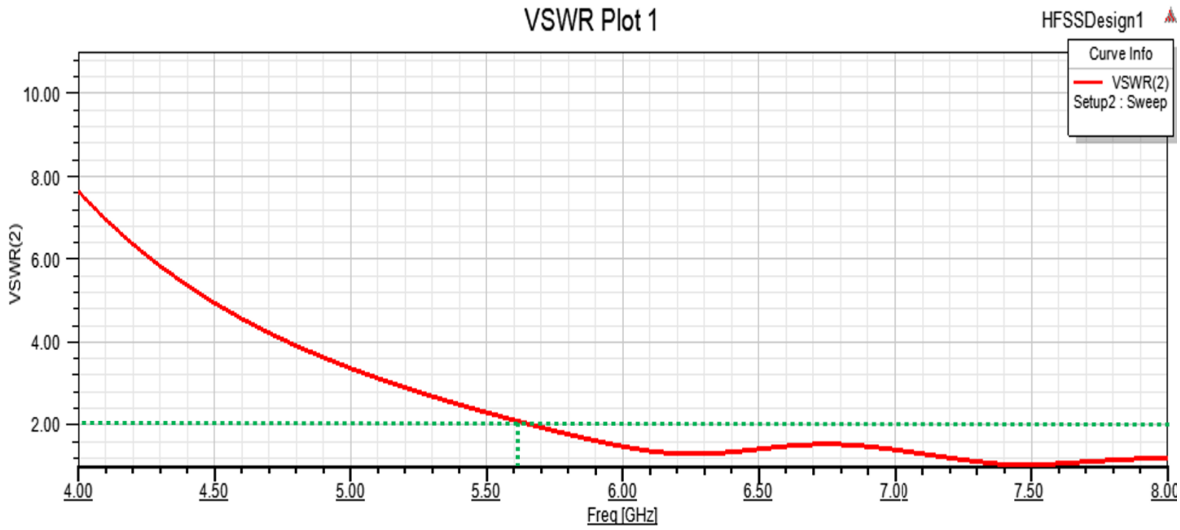

Figure 3.13: VSWR plot of bowtie dipole antenna

The VSWR plot above shows that the antenna has a viable performance after 5.6 GHz as the SWR falls below 2 dB. This low value indicates that there is less impedance mismatch. Less power is reflected and as a result, a better power transfer is achieved. There are some slight discrepancies between these results and that of the referenced antenna.

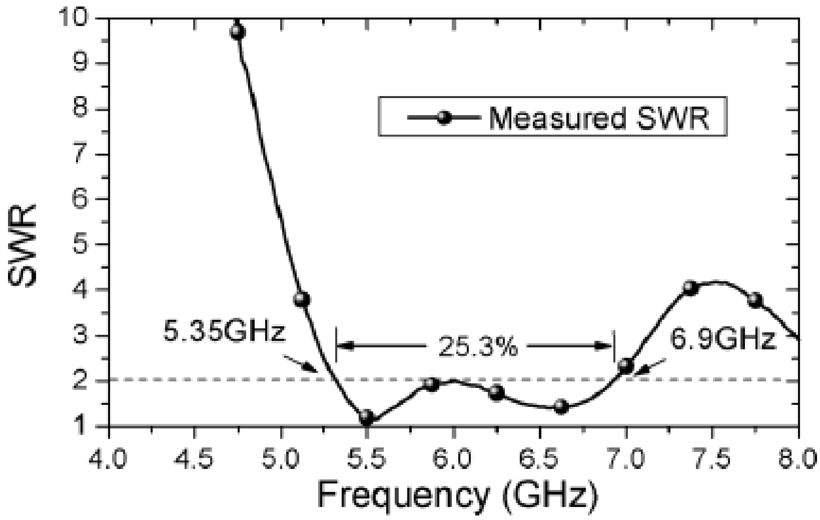

Figure 3.14: VSWR plot of reference bowtie dipole antenna

The reference antenna is able to achieve an SWR of less than 2 dB at the 5.35 GHz mark which is 0.25 GHz lower than the frequency at which the aforementioned antenna hits the 2 dB mark.

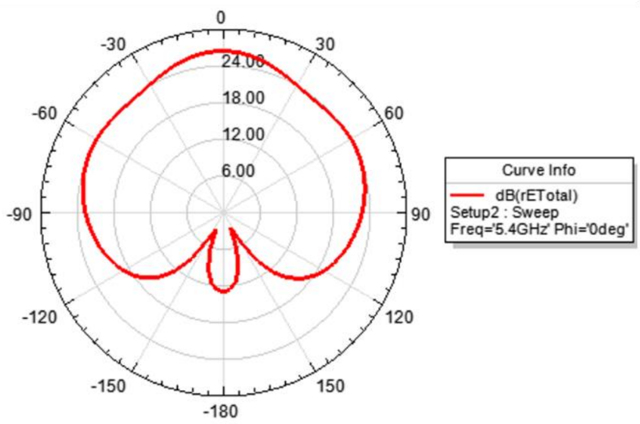

Figure 3.15 Designed antenna: 5.4 GHz

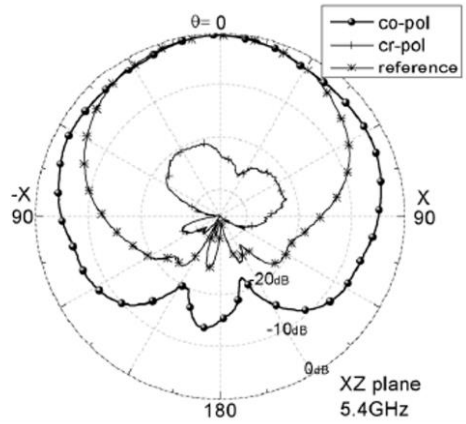

Figure 3.16 Reference antenna: 5.4 GHz

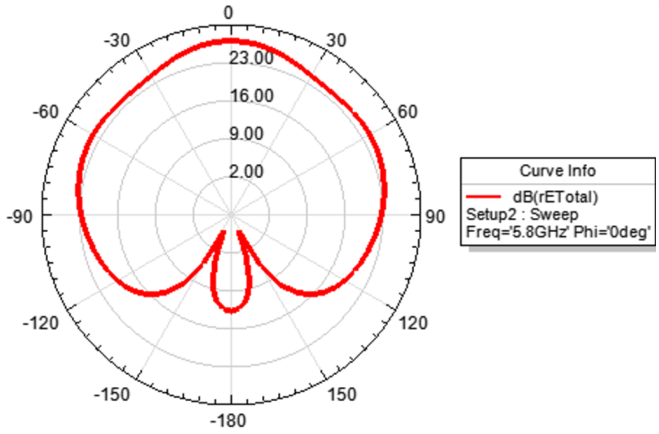

Figure 3.17 Designed antenna: 5.8 GHz

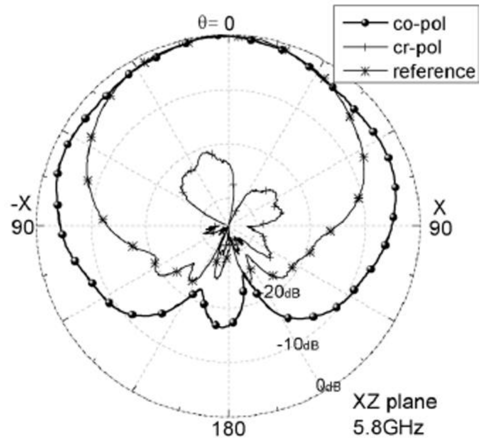

Figure 3.18 Reference antenna: 5.8 GHz

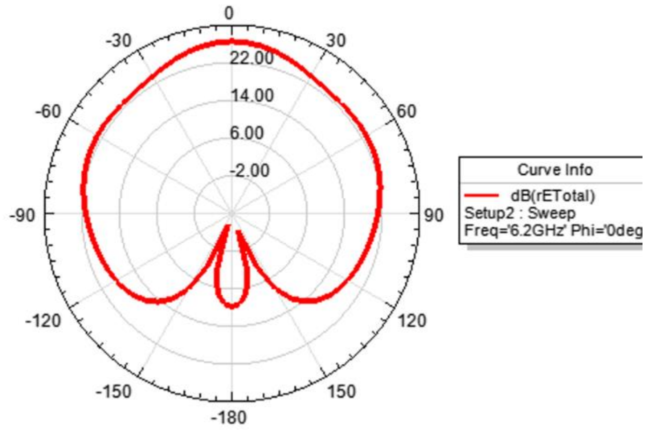

Figure 3.19 Designed antenna: 6.2 GHz

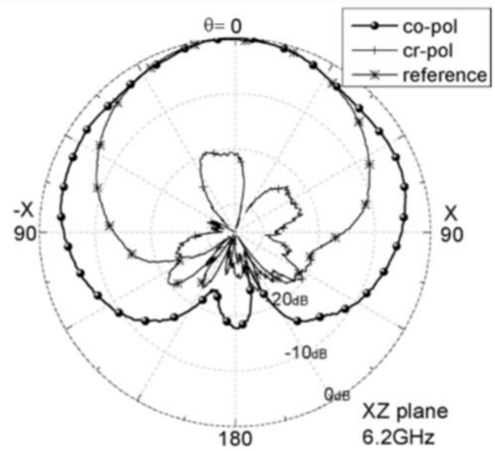

Figure 3.20 Reference antenna: 6.2 GHz

The radiation patterns above show the H-plane radiation pattern of the designed bowtie dipole antenna on the left and the referenced bowtie antenna on the right – at frequencies of 5.4 GHz, 5.8 GHz and 6.2 GHz respectively. For the patterns on the right, the outermost patterns should be observed as the inner ones are results obtained when the metallic bridge is removed. As can be seen from the figures above, the radiation patterns of the referenced antenna are slightly wider than that of the antenna designed for this project. This could be due to some minor physical discrepancies between the 2 antennas.

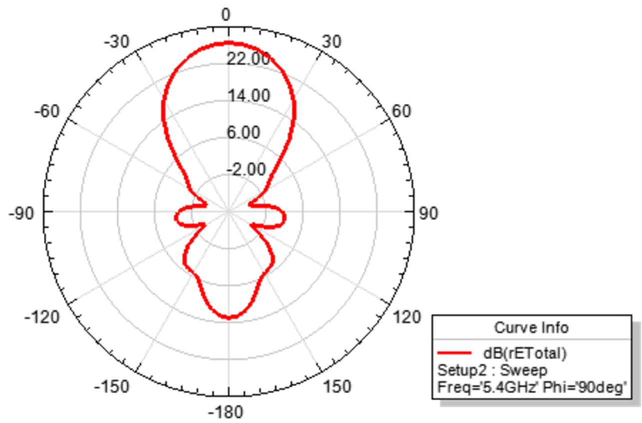

Figure 3.21 Designed antenna: 5.4 GHz

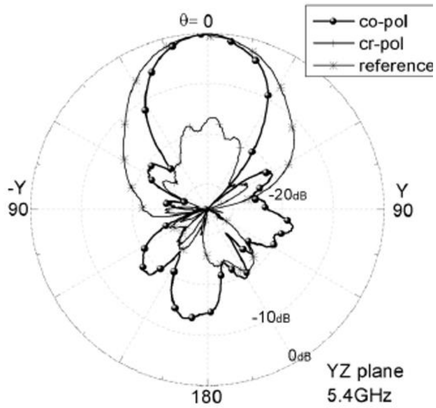

Figure 3.22 Reference antenna: 5.4 GHz

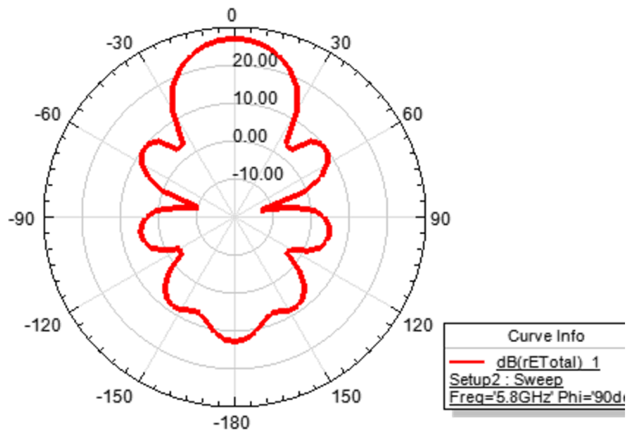

Figure 3.23 Designed antenna: 5.8 GHZ

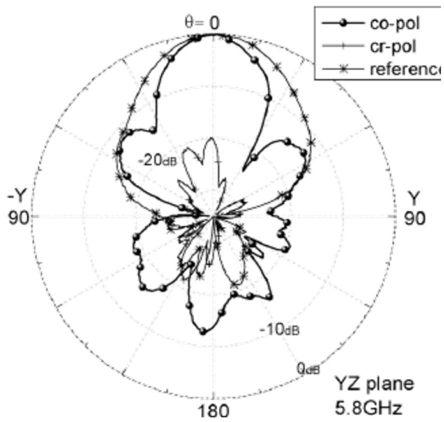

Figure 3.24 Reference antenna: 5.8 GHz

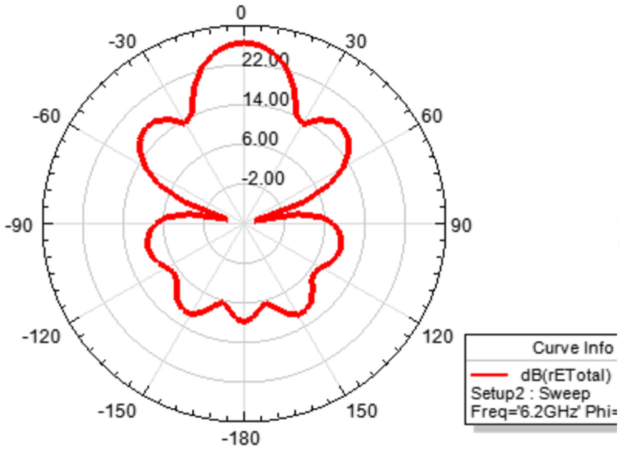

Figure 3.25 Designed antenna: 6.2 GHz

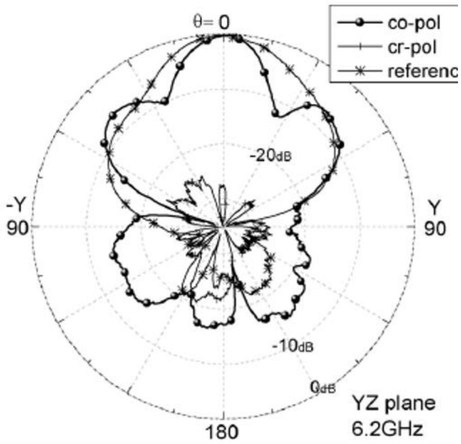

Figure 3.26 Reference antenna: 6.2 GHz

The radiation patterns above show the E-Plane radiation pattern of the designed antenna on the left and the referenced one on the right. The radiation pattern lines labelled as co-pol should be observed for the diagrams on the right. The E-plane patterns for both antennas are similar at the different frequencies, with slight discrepancies.

Chapter 4

Our Proposed Antenna

In this chapter, the process of designing a UHF low-profile antenna will be detailed and the results of its simulation will be presented. The antenna will be one that operates over the frequency range of 200 to 600 MHz. The antenna presented in Chapter 3 will be scaled to a size that will allow it to operate within this frequency range.

Following this, loading techniques can be studied in order to obtain a substantial reduction of the size and profile of the antenna.

4.1 Scaling of the Antenna

The metallic bridge of the antenna system and its two copper supports, with ends attached to the ground plane, were removed and the antenna was once again simulated with all other physical parameters and design kept intact. This antenna was then assigned the same excitation with a lumped port of impedance 100 Ω. The results of this simulation is shown in the figures below.

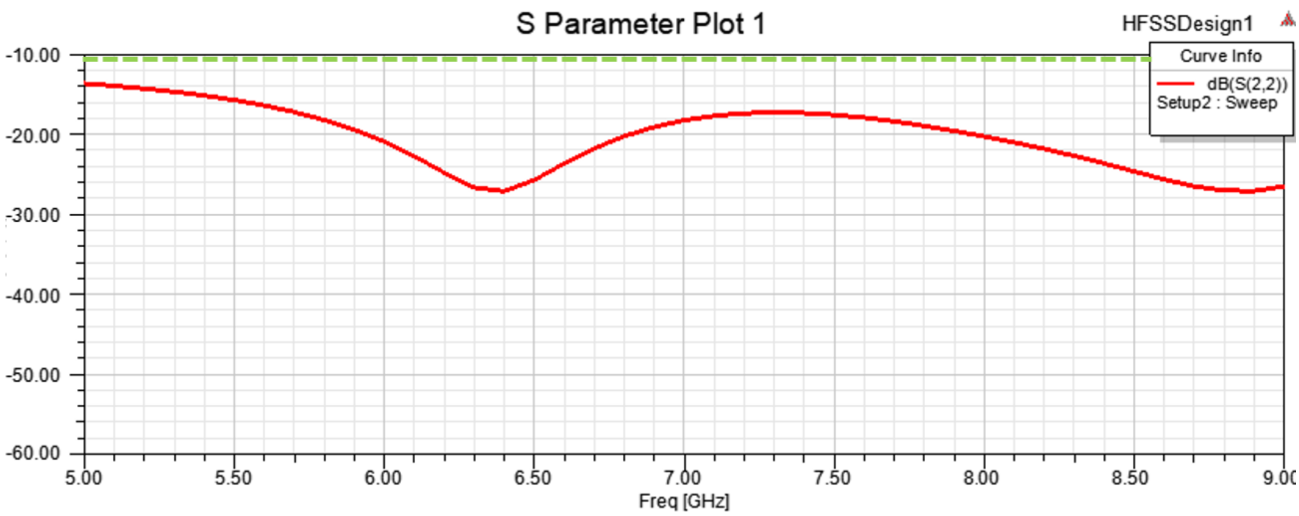

Figure 4.1: S-parameter plot of antenna without metallic bridge

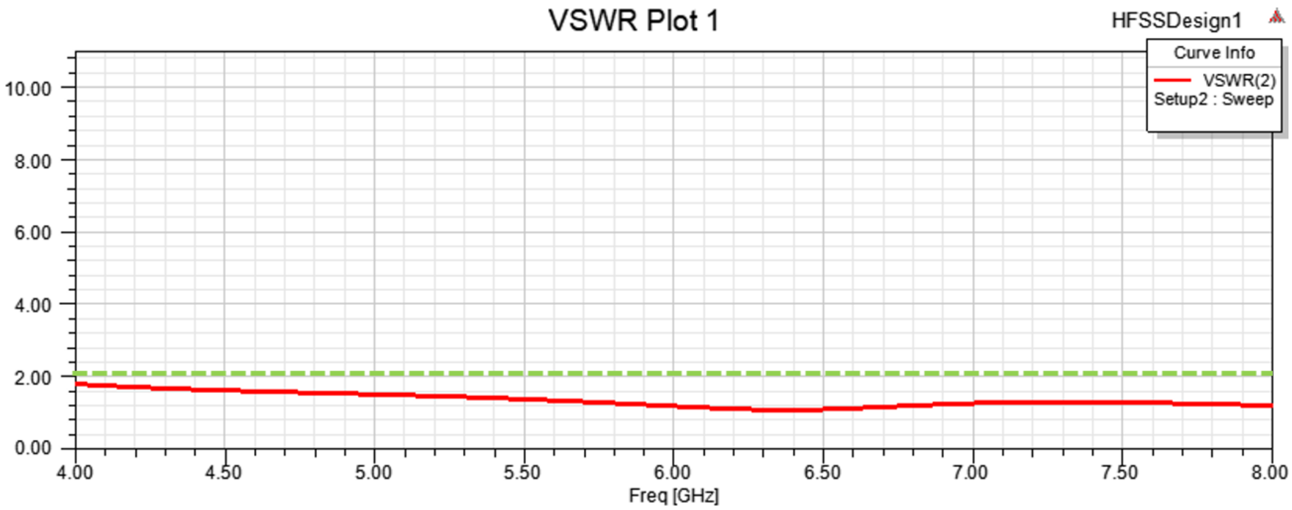

Figure 4.2: VSWR plot of antenna without metallic bridge

The figures above indicate that the return loss falls below 10 dB and the VSWR is below 2 dB. These results verify that the antenna is still viable without the metallic bridge placed over the bowtie dipole and therefore, it will be removed for this part of the project for the sake of simplicity.

The bow-tie antenna is a form of half-wavelength dipole antenna and therefore, the wavelength of the antenna and the dimensions of the bowtie element are related via the following equation [25]:

$$Width = \frac{\lambda}{2} \tag{13}$$

Since the desired operational frequency begins at 200 MHz, the wavelength and subsequently, the width of each arm of the bowtie, can be calculated as follows.

$$\Lambda = \frac{c}{f} = \frac{300000000}{200000000} = \frac{3}{2}m = 1500mm \tag{14}$$

$$width \;\; of\, bowtie\, element = \frac{1500}{2} = 750mm \tag{15}$$

$$width \;\; of\, each\, bowtie\, arm = \frac{750 - 1}{2} = 374.5mm \tag{16}$$

The width of the entire bowtie element is derived to be 750 mm. This correlates to a scaling factor of 15 times as compared to the physical dimensions of the antenna presented in chapter 3.

The width of each arm in the bowtie would be 374.5 mm as there will be a lumped port in the centre gap of width 1mm. The dimensions of the rest of the design (the ground plane) was scaled to 15 times as well and the resultant design is presented below. The surrounding cuboid is a radiation boundary with an inner offset of 12mm at each face.

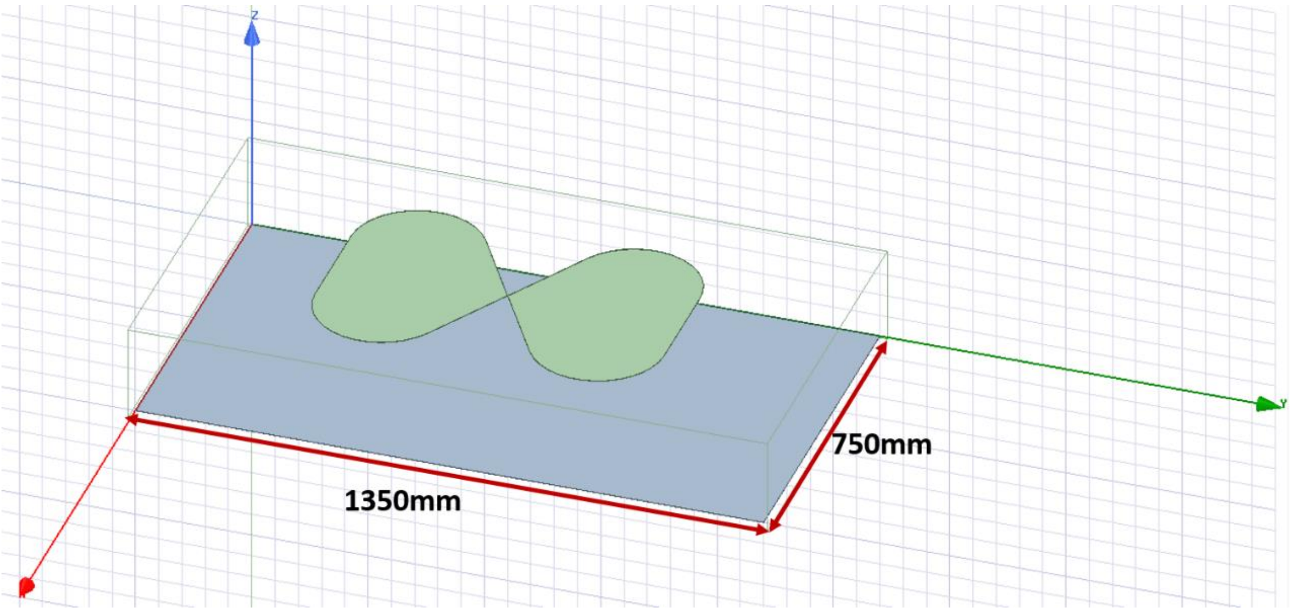

Figure 4.3: Dimensions of scaled ground plane

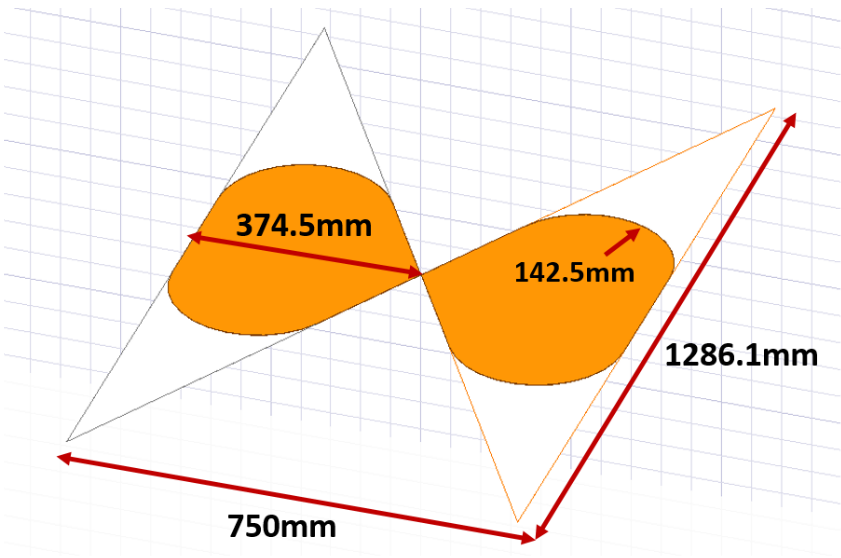

Figure 4.4: Dimensions of scaled bowtie element

The height of the antenna with relation to the ground plane has also been adjusted according to the scale factor. The new height is now 187.5 mm.

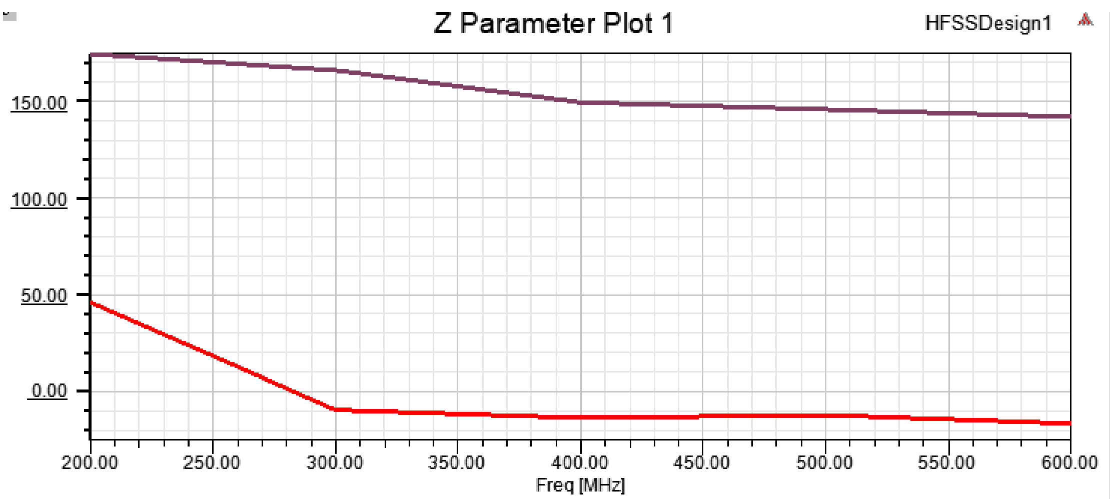

Figure 4.5: Z-parameter plot

The Z-parameter plot was then retrieved in order to determine the impedance of the lumped port situated in the centre gap of the bowtie element. The plot above shows the real and imaginary impedances of the simulated antenna.

$$Z_{in} = R_{in} + jX_{in}, \quad Z_0 = R_{in} \tag{17}$$

As shown above in equation (17), input impedance is equivalent to the real and imaginary impedances of an antenna. The characteristic impedance is made up of only the real part of the input impedance. The Z-parameter plot shows that the real impedance of the antenna is 175 Ω when the imaginary value is 0 Ω and therefore, this value was set to be the port impedance.

4.2 Results and discussion

The performance results of the scaled antenna is as follows:

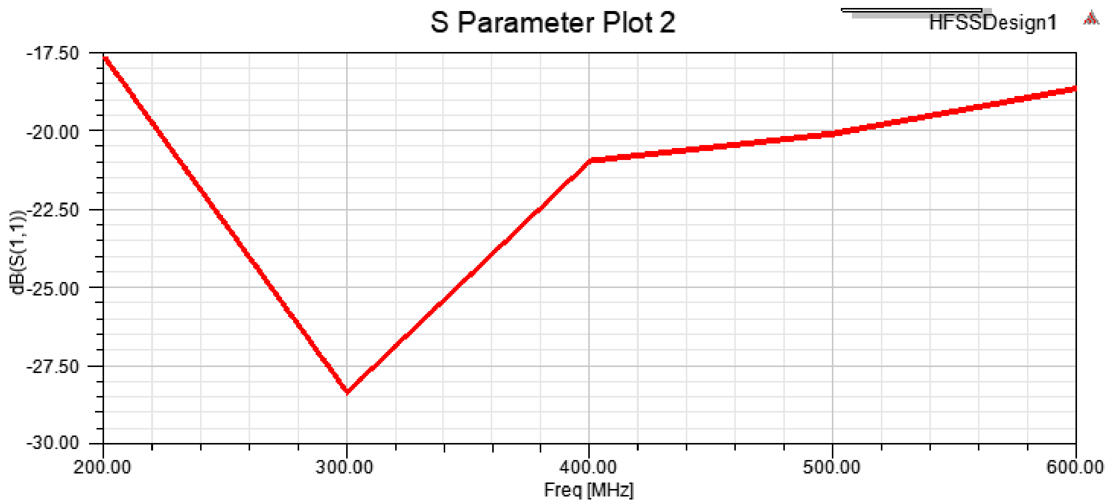

Figure 4.6: S-Parameter plot

Since the S_{11} plot above falls below -10 dB for all the points in the frequency sweep, the return loss for this antenna can be considered to be favourable.

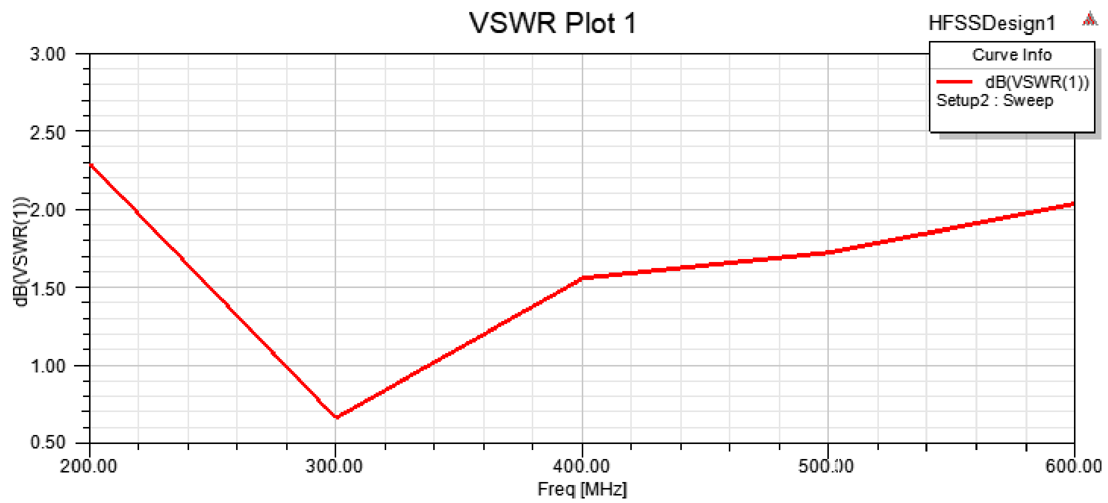

Figure 4.7: VSWR plot

The VSWR shows that there is little impedance mismatch for the antenna as the plot falls below 2 dB for frequency values after 218 MHz till 600 MHz.

The radiation patterns for the antenna at frequencies of 300 MHz, 400 MHz, 500 MHz and 600 MHz are shown below. On the left are the plots for the radiation observed in the E-plane and on the right are the plots for radiation observed in the H-plane.

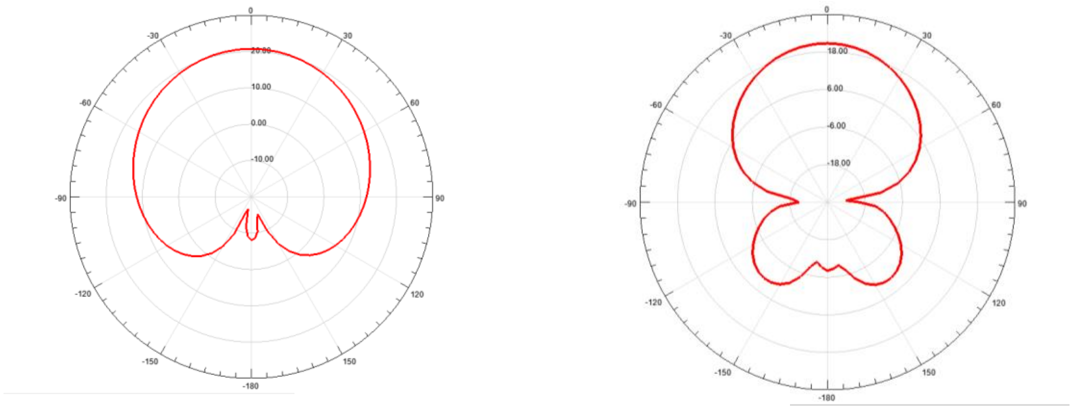

Figure 4.8: Radiation patterns at 0.3 GHz

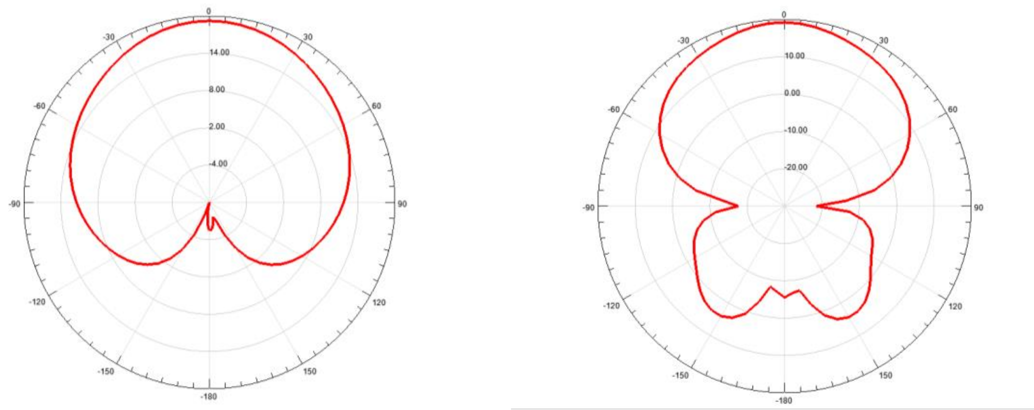

Figure 4.10: Radiation patterns at 0.4 GHz

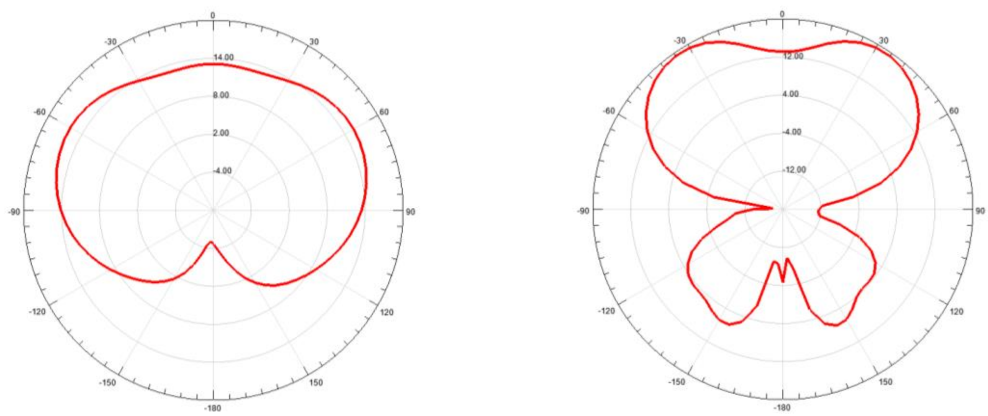

Figure 4.9: Radiation patterns at 0.5 GHz

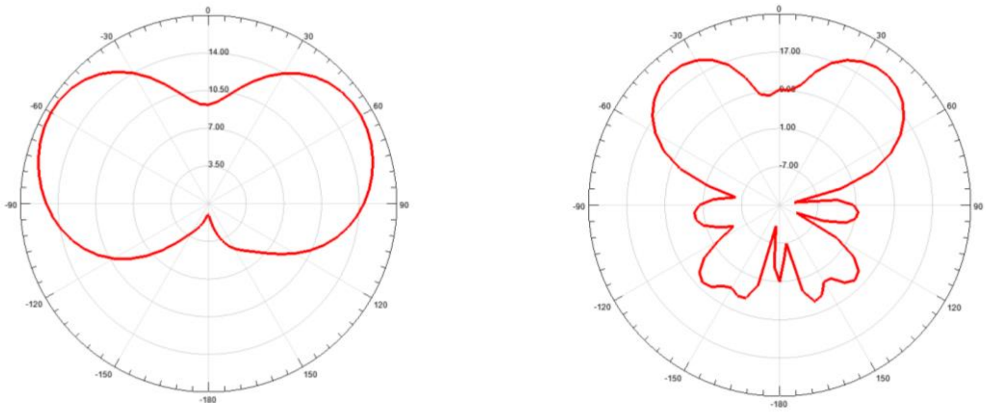

Figure 4.11: Radiation patterns at 0.6 GHz

The above patterns show that gain of the antenna decreases as the frequency increases. Since the VSWR and S-parameter plots have proven the scaled antenna to be viable, this antenna can be used for further studies of miniaturization techniques to achieve a reduced profile antenna.

4.3 Magneto-Dielectric materials for antenna miniaturization

A possible method of miniaturization for the aforementioned antenna could be the loading of the system with magneto-dielectric materials. Magneto-dielectric materials are typically ceramic or composite materials with a controller relative permeability and relative permeability that are both greater than one. For starters, increasing a composite material's magnetic permeability will increase the intrinsic impedance of said material. Since the refractive index of a material can be computed using the square root of permittivity multiplied by permittivity, having a permeability value of above one allows a larger refractive index to be achieved. [28]

The type of material used depends on the operating frequency of the antenna. For UHF antennas, ferrite materials are typically used. In the frequency range from 100 MHz to 700 MHz, the material known as spinel ferrite has a permeability of 4.8-5.9 and a permittivity of around 4.1-j0.05 [29] and these are considered to be good electromagnetic properties that exhibit great potential for miniaturization of antennas in the UHF frequency band. By increasing the intrinsic impedance of the material while increasing the refractive index, one can obtain a material that produces a smaller antenna at an impedance that allows it to operate at almost the same bandwidth as before [28].

This method can be realized by making physically small antennas from ferrite substrates. When an electromagnetic wave propagates through a medium, this medium will cause the wave to slow down at a rate that is equivalent to the refractive index [29].

$$n = \sqrt{\varepsilon\mu} \tag{18}$$

Where n = refractive index, ε = permittivity, μ – permeability

A large n will reduce the wavelength of the electromagnetic wave in the material by an increased amount. In addition, the material will have an intrinsic impedance, which is also a function of permeability and permittivity, except that it is related by ratio instead of product. Therefore, it can be inferred that a material that has a high permittivity will have a high refractive index and a low intrinsic impedance. In the instance in which a wave is propagating between two mediums, the impedance discontinuity results in a reflectance or reflection at the interface.

For example, take into consideration a dielectric material that has a dielectric constant of 36 and a magneto-dielectric material that has ε and μ both of value 6. If an antenna has been fabricated on both substrates, the one built on the magneto dielectric material would a bandwidth that is larger by almost 6 times. These performance enhancements are a reason why magneto-dielectric materials can be used to miniaturize an antenna. The bowtie dipole antenna presented in this report can be fabricated on a magneto-dielectric ferrite material with ε and μ values that are above 1instead of being fabricated on a dielectric material with dielectric constant of 2.65 [29]. Considerable reduction of antenna dimensions can then be achieved due to the properties of magneto-dielectric materials that have been discussed in this section. Due to time constraints, the author was not able to use HFSS to successfully fabricate and simulate an antenna with a suitable magneto-dielectric substrate, but it is surely a potential avenue that should be considered for future work.

Chapter 5

Conclusion

5.1 Summary of Work Conducted

As discussed in this report, the work conducted to achieve this project's objectives include the construction of a bowtie dipole antenna that performs in the super-high frequency range of 5-6 GHz, the scaling of said antenna to allow it to operate in the ultra-high frequency range of 200-600 MHz, and the study of a miniaturization technique to further reduce the size of the antenna. These undertakings were conducted in an attempt to design a low-profile antenna that can operate within an ultra-high frequency band.

The project heavily involved the use of the simulation software known as HFSS and this software allowed for the analysis of the performance results of the aforementioned antennas. Extensive readings about antenna systems and their parameters was done throughout the duration of this project and this aided in the interpretation of the results obtained from the HFSS simulations.

Overall, this project has been very fulfilling. During the course of this project, the author has picked up valuable experiences and skill sets that aid in the understanding of how antennas operate. The author has also gained much knowledge about the intricacies of "small antenna" design, UHF low-profile antennas and has acquired enough familiarity with HFSS to fabricate and simulate antennas. Although substantial reduction for the physical size of the antenna has not been achieved in this project, the design presented serves as a basis to which more improvements can be made in order to obtain miniaturization and performance enhancements.

5.2 Recommendation for Future Work

Further work can be done in order to design a viable and well-performing low-profile wideband antenna and to contribute to the discourse on the design of small antennas. To improve on this project, additional miniaturization techniques should be employed in order to further reduce the size of the antenna while protecting its performance from degradation. One such technique would be to load the antenna system with magneto-dielectric materials for reasons that have been discussed in section 4.3 of this report.

Changes to the physical configuration of the antenna can also be carried out in an attempt to make the antenna system more compact. For example, it would be useful to compute a method that can derive the maximum fillet radius of the rounded corners of the bowtie before performance degradation begins.

References

[1] A. Ghose and S. Pil Han, "Estimating Demand for Mobile Applications in the New Economy", *Pdfs.semanticscholar.org*, 2013. [Online]. Available:https://pdfs.semanticscholar.org/a45a/.pdf.

[2] H. Kogure, Y. Kogure and J. C. Rautio, *Introduction to Antenna Analysis Using EM Simulators*. Tokyo, 2011, p. 3.

[3]S. Hu and D. Tanner, "Building Smartphone Antennas That Play Nice Together", *IEEE Spectrum*, 2018. [Online]. Available: https://spectrum.ieee.org/telecom/wireless/building-smartphone-antennas-that-play-nice-together.

[4] K. Fujimoto, A. Henderson, K. Hirasawa and J. James, *Small Antennas*. 1987.

[5] M. Hirvonen, "Performance Enhancement of Small Antennas and Applications in RFID", 2008.

[6] E. Notes, "Antenna Theory | Aerial Basics | Electronics Notes", *Electronics-notes.com*. [Online]. Available: https://www.electronics-notes.com/articles/antennas-propagation/antenna-theory/basics-tutorial.php.

[7] P. Bevelacqua, "Antenna Basics", *Antenna-theory.com*. [Online]. Available: http://www.antenna-theory.com/basics/main.php

[8] G. Raju, "Antennas and Wave Propagation", *Google Books*, 2009. [Online]. Available: https://books.google.com.sg/books/

[9] "Antenna Theory Tutorial - Tutorialspoint", *Tutorialspoint.com*. [Online]. Available: https://www.tutorialspoint.com/antenna_theory/index.htm.

[10] T. Agarwal, "Different types of Antennas with Properties and their Working", *ElProCus - Electronic Projects for Engineering Students*. [Online]. Available: https://www.elprocus.com/different-types-of-antennas-with-properties-and-thier-working/

[11] "Log-periodic antenna", *En.wikipedia.org*. [Online]. Available: https://en.wikipedia.org/wiki/Log-periodic_antenna

[12] "VAS UHF 900 MHz Semi-rigid Dipole Antenna", *English*. [Online]. Available: https://www.getfpv.com/vas-uhf-900-mhz-semi-rigid-dipole-antenna.html.

[13] R. Pearce, *Yagi-Uda Antenna Array*. 2019.

[14] J. Lienau, "Understanding Antenna Design", *Laird Connect*, 2019. [Online]. Available:

https://www.lairdconnect.com/resources/white-papers/understanding-antenna-design.

[15] "What is meant by the VSWR of an antenna? - MobileMark", *MobileMark*, 2019. [Online]. Available: https://www.mobilemark.com/about/faq/what-is-meant-by-the-vswr-of-an-antenna/.

[16] P. Bevelacqua, "Antenna Arrays: Performance Limits and Geometry Optimization", *Antenna-theory.com*, 2008. [Online]. Available: http://www.antenna-theory.com/Bevelacqua-Dissertation.pdf.

[17] S. Smiley, "RFID Antennas: Beamwidth & Directivity - RFID Insider", *RFID Insider*, 2016. [Online]. Available: https://blog.atlasrfidstore.com/rfid-antennas-beamwidth-directivity.

[18] Asmadi, "Aircraft Communication Modulation and propagation of radio waves", *Slideshare.net*. [Online]. Available: https://www.slideshare.net/alexantrine92/topic-2-modulation-and-propagation-of-radio-waves.

[19] "Ultra high frequency", *En.wikipedia.org*. [Online]. Available: https://en.wikipedia.org/wiki/Ultra_high_frequency.

[20] J. Diot et al., "A Novel Antenna for Transient Applications in the Frequency Band 300 MHz – 3 GHz: The Valentine Antenna", *Semanticscholar.org*, [Online]. Available: https://www.semanticscholar.org/paper/A-Novel-Antenna-for-Transient-Applications

[21] "Biconical antenna", *En.wikipedia.org*. [Online]. Available: https://en.wikipedia.org/wiki/Biconical_antenna.

[22] S. Qu, J. Le-Wei Li and Q. Xue, "Bowtie Dipole Antenna With Wide Beamwidth for Base Station Application", 2007. [Online]. Available: https://www.researchgate.net/publication/

[23] S. Qu and C. Ruan, "Effect of Round Corners on Bowtie Antennas", *Pdfs.semanticscholar.org*, 2006. [Online]. Available: https://pdfs.semanticscholar.org/eceb/pdf.

[24] J. Munn, "Your Guide to Lumped Ports in the RF Module", *COMSOL Multiphysics*. [Online]. Available: https://www.comsol.com/blogs/your-guide-to-lumped-ports-in-the-rf-module/.

[25] T. Jun, "Design of a Multiband Antenna", Singapore, 2019.

[26] D. Pinchera, M. Donald Migliore, F. Schettino and G. Panariello, "An Effective Compressed-Sensing Inspired Deterministic Algorithm for Sparse Array Synthesis", 2017. [Online].

[27] "Bowtie Antenna basics | Bowtie Antenna Calculator", *Rfwireless-world.com*. [Online]. Available: https://www.rfwireless-world.com/calculators/Bowtie-Antenna-Calculator.html.

[28] K. Sprentall, *Introduction to Magneto-Dielectric Materials for Antenna Miniaturization*. 2019.

[29] G. Le Fur, F. Grange and C. Leveaud, "Contribution on notch antenna loaded by magneto-dielectric material", 2011. [Online]. Available: https://www.researchgate.net/publication/Contribution_on_notch_antenna_loaded_by_magneto-dielectric_material.